Task 4.1

Title

Risk, safety and societal acceptance

Projects (presented on the following pages)

A preliminary Spatial Multi-Criteria Decision Analysis for Deep Geothermal Systems in Switzerland
Alternative: Task 4.2
M. Spada, P. Burgherr

Building informed and realistic public preferences for Swiss electricity portfolios
S. Volken, G. Xexakis, E. Trutnevyte

Are Interactive Web-Tools for the Public Worth the Effort? An Experimental Study on Public Preferences for the Swiss Electricity System Transition
G. Xexakis, E. Trutnevyte

SCCER SoE
SWISS COMPETENCE CENTER for ENERGY RESEARCH
SUPPLY of ELECTRICITY

SCCER-SoE Annual Conference 2017

In cooperation with the CTI
Energy
Swiss Competence Centers for Energy Research
Schweizerische Eidgenossenschaft
Confédération suisse
Confederazione Svizzera
Confederaziun svizra
Swiss Confederation
Commission for Technology and Innovation CTI

Hierarchical Bayesian Modelling for Fluid-Induced Seismicity

Marco Broccardo, Arnaud Mignan, Bozidar Stojadinovic, Stefan Wiemer, and Domenico Giardini.

Abstract

A key component of the risk governance framework for induced seismicity arising from fluid-induced injections is the definition of a set of risk mitigation strategies. Among the possible strategies, Traffic Light Systems (TLS) are frequently used to mitigate induced seismicity risk by modifying the fluid injection profile. Shortly, a TLS defines one decision variable (event magnitude, peak ground acceleration, etc.) and a series of safety thresholds above which injection should be modified or eventually stopped. This poster presents the ground for a TLS based on a Bayesian Hierarchical model. Briefly stated, a hierarchical Bayesian model utilizes multistage prior distributions of the model parameters. A major strength of the Bayesian approach is that it allows uncertainties and information about parameters to be encoded into a joint prior distribution of the model parameters. Moreover, it allows the computation of posterior predictive distribution of the model parameters as soon as the project is started and information becomes available.

Probabilistic model

The recurrence of earthquake events is modeled with a non-homogeneous Poisson process (NHPP), defined by time varying rate $\lambda(t)$. The rate model is given as

$$\lambda(t;\boldsymbol{\theta}) = \begin{cases} 10^{a-bm_0}\dot{V}(t) & t \le t_s \\ 10^{a-bm_0}\dot{V}(t_s)\exp\left(-\frac{t-t_s}{\tau}\right), & t > t_s \end{cases}$$

where $\dot{V}(t)$ is the injection rate and t_s the shut in time, a the activation feedback, b the earthquake size ratio, and τ the mean relaxation time.

Figure 1 shows samples of the NHPP for a given set of parameters

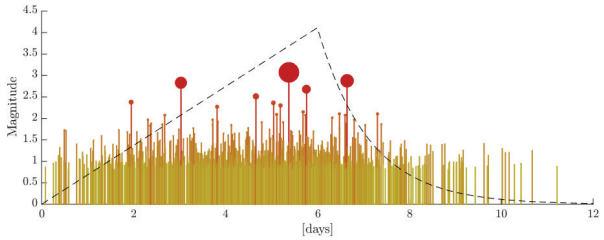

Figure 1 Sample of seismic induced sequence for given values of a, b and τ

Bayesian Hierarchical model, definition and inference

In a Bayesian approach, we consider a, b and τ as random variables adding an extra layer of uncertainty. The prior parameters distribution aim to reflect the relative likelihood of its possible outcomes, taking into account the uncertainties before gathering observations. We can represent models such as this one via Bayesian networks—also known as directed cyclic graph (DAG). Figure 1 shows the proposed model.

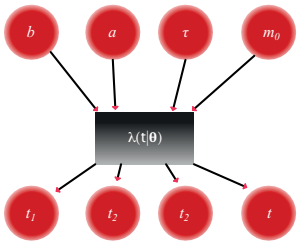

Figure 2 DAG for the proposed Bayesian hierarchical model

As standard practice in DAG, we denote with nodes the random variables, and with a box the model that encode the physics of the problem. From Figure 2, one can observe that the proposed framework is generalizable for any rate model different from the one recommended in this poster. The selection of the prior is the controversial part of Bayesian statistics since it is not unique and can be subject to personal interpretation. However, this can also be viewed as a strength since it allows experts to constrain the domain of the hyper-parameters by encoding physical principles and evidence. In this poster, we choose a subjective prior distribution, since the available data are limited to few past events, and we cannot gather in-situ information before a project take place. Figure 3 shows the three prior distributions, which are Beta distribution for a and b, and the Gamma distribution for τ. The classical Bayesian inference is used to update the probability distribution of the hyper-parameters when observations are available.

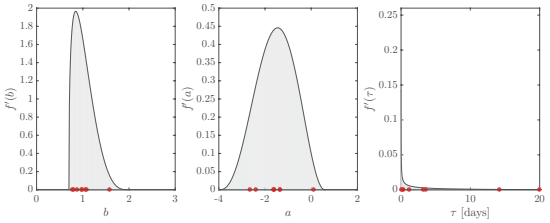

Figure 3 Prior distribution for a, b and τ

Given a set of observations, $D = [t_1, \dots, t_N; m_1, \dots, m_N]$, we update the probability distribution of the hyper-parameters as follo$f''_{\boldsymbol{\theta}}(\boldsymbol{\theta}|\mathcal{D}) = c\mathcal{L}(\mathcal{D}|\boldsymbol{\theta})f'(\boldsymbol{\theta})$
The likelihood is derived as:

$$\mathcal{L}(\mathcal{D}|\boldsymbol{\theta}) = \left[\prod_{n=1}^{N}\frac{\lambda(t_n|\boldsymbol{\theta})}{\Lambda(T)}f_M(m_n|b)\right]\Lambda^N(T|\boldsymbol{\theta})\exp\left[-\Lambda(T|\boldsymbol{\theta})\right] = \left[\prod_{n=1}^{N}\lambda(t_n|\boldsymbol{\theta})f_M(m_n|b)\right]\exp[-\Lambda(T|\boldsymbol{\theta})]$$

where $\Lambda(t) = \int_0^t \lambda(t')dt'$

The small parameter space enable numerical integration. Figure 4 shows: in the diagonal the prior marginal distribution and the posterior marginal distribution of the parameters; in the lower triangular part, the prior pair-wise distribution; and in the upper triangular part, the posterior pair-wise di

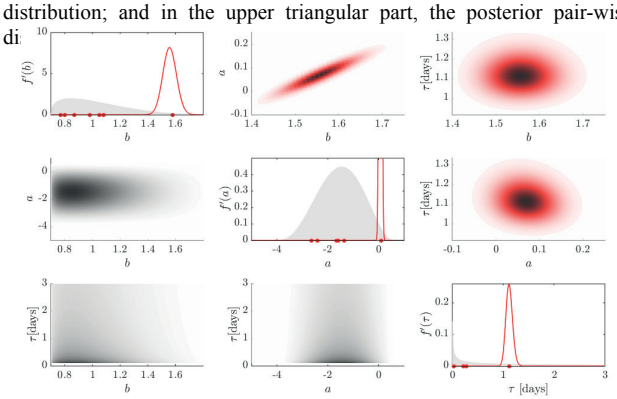

Figure 4 Posteriors distributions of a, b and τ

Anticipation model, predictive distribution

The proposed Bayesian model also allows a precise classification of the uncertainties. In particular, we separate epistemic (encoded in the parameter distributions) from aleatory uncertainty (encoded in the Poisson model). This separation is important in the prediction model which is derived as fi

$$P(N(t\in[t+h])=n|\mathcal{D}(t)) = \int_{\boldsymbol{\theta}}\left[\frac{\int_t^{t+h}\lambda(t'|\boldsymbol{\theta})dt'}{n!}\exp\left[-\int_t^{t+h}\lambda(t'|\boldsymbol{\theta})dt'\right]\right]f''_{\boldsymbol{\theta}}(\boldsymbol{\theta}|\mathcal{D}(t))d\boldsymbol{\theta}$$

Figure 5 shows prediction and true outcome for a window time of 4 hours

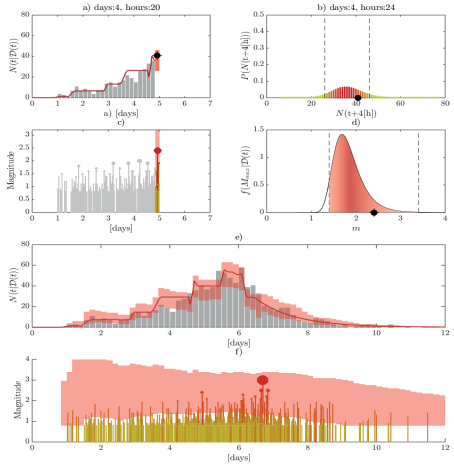

Figure 5 Anticipation model: left rates, right probability distribution of number of seismic events

SCCER-SoE Annual Conference 2017

SCCER SoE
SWISS COMPETENCE CENTER for ENERGY RESEARCH
SUPPLY of ELECTRICITY

In cooperation with the CTI
Energy
Swiss Competence Centers for Energy Research
Schweizerische Eidgenossenschaft
Confédération suisse
Confederazione Svizzera
Confederaziun svizra
Swiss Confederation
Commission for Technology and Innovation CTI

70 NRP Energy Turnaround
National Research Programme

PAUL SCHERRER INSTITUT
PSI

(FRS) FUTURE RESILIENT SYSTEMS 未来韧性系统

Transformation of the Energy-related Severe Accident Database (ENSAD) into an interactive, web-based GIS application

P. Burgherr[1], W. Kim[2], M. Spada[1], A. Kalinina[1], S. Hirschberg[1]
[1]Technology Assessment Group, Paul Scherrer Institut, Villigen PSI, Switzerland
[2]Future Resilient Systems (FRS) , Singapore-ETH Centre, Singapore

Introduction

The **risk assessment of energy technologies** is a mature and established scientific field with a strong quantitative foundation (*Burgherr & Hirschberg, 2014*). Numerous important conceptual and methodological achievements since the 1980s continuously advanced its state-of-the-art. Particularly in the past two decades a more **integrated perspective** on risk assessment has emerged by combining it with several overarching concepts such as **sustainability**, **energy security**, **critical infrastructure protection** and **resilience**.

The systematic and **comprehensive collection of historical accidents** in the energy sector requires that complete energy chains are considered because accidents can occur at all stages and not just during the actual power and/or heat generation. However, such a dedicated and authoritative database became only available with the establishment of the **Energy-related Severe Accident Database** (**ENSAD**) by the Paul Scherrer Institut (PSI) in the 1990s (*Hirschberg et al., 1998*).

Current status of ENSAD

ENSAD has a number of advantages compared to general industrial and specialized ("narrow-scope") databases, including a **broad application range** with regard to accident risk assessment in the energy sector (*Burgherr et al., 2017*). Despite these obvious advantages, continuous improvements and developments, ENSAD has remained a static, non-spatial database in MS Access format. Therefore, a completely new, **interactive, web-based GIS database** – **ENSAD v2.0** – is developed with the following features:

1. **Spatial database** for accidents involving energy infrastructures.
2. Geo-referenced data based on **advanced geo-coding** technology.
3. **Web-based Geographic Information System** (GIS) to visualize and analyze the spatial and temporal characteristics of accidents.

Structure and Features of ENSAD v2.0

Figure 1 shows the system architecture and data flow of the new ENSAD v2.0, which is based on a **cloud server and open-source technologies**. The connection to a GIS server (GeoServer) generates the map content for the web client that meets the OGC (Open Geospatial Consortium) standard, i.e. WMS (Web Map Services), WFS (Web Feature Service), etc. ENSAD v2.0 is developed as a **responsive web application** so that a user can access it from a PC as well as a mobile device such as smartphone or tablet.

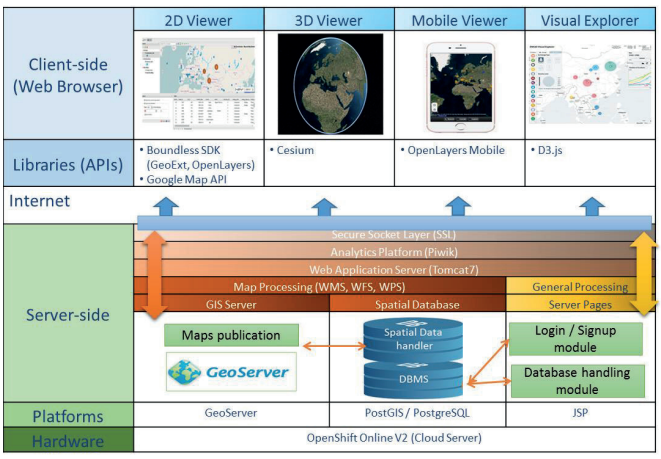

Figure 1: System architecture and data flow of ENSAD v2.0 (*Kim et al, 2017*).

On the client side, four ENSAD v2.0 versions are available. The **desktop version** provides the **complete information for all 32'963 accidents**, and data can be visualized either in 2D or 3D (**Figure 2, left**). Due to its limited screen size, the **mobile version focuses on displaying specific accident information** only. Users can also check for accident information at their current location using the positioning capabilities of their mobile device. Finally, the so-called **ENSAD Visual Explorer (EVE)** provides a **public version** of ENSAD v2.0 with access to a **limited number of data fields**, but all accident records can be viewed on a world map and pre-defined visualizations as well as limited analysis capabilities are available (**Figure 2, right**).

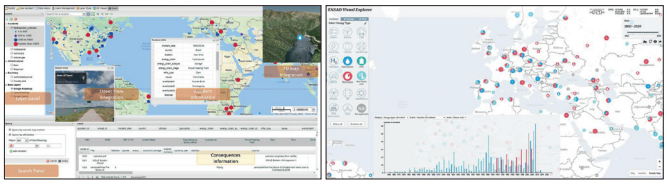

Figure 2: Main interfaces of ENSAD v2.0 desktop version (**left**), and ENSAD Visual Explorer (**right**) (*Kim et al., 2017*).

Selected Case Study Applications of ENSAD v2.0

Figure 3 shows two **case study examples using ENSAD v2.0**, namely **(left)** risk assessment of dam accidents, and **(right)** rough set analysis to develop classification models for natural gas accidents. Other ongoing activities include (1) the analysis of potential impacts of selected natural hazards and technical failures on the European natural gas transmission network and its recovery dynamics (e.g. *Kyriakidis et al., 2017*), and (2) the development of a web scraping tool to facilitate future updates of ENSAD with new energy accident data.

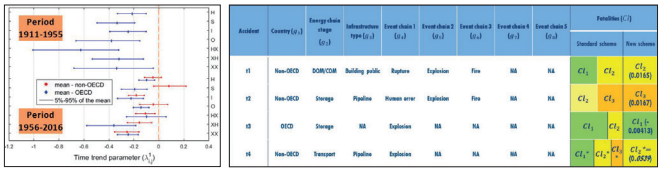

Figure 3: ENSAD v2.0 case study examples. (**left**) dam risk assessment (*Kalinina et al., 2016*), (**right**) rough set analysis (*Cinelli et al., 2017*).

Acknowledgments

This work has been carried out within the **Swiss Competence Center on Energy Research – Supply of Electricity** (concept, data management and preparation of data migration), the **Energy Turnaround National Research Programme (NRP70)** of the Swiss National Science Foundation (dam accident prototype), and the **Future Resilient Systems (FRS) program** of the Singapore-ETH Centre (SEC) (tool development and implementation, data migration).

References

- Burgherr, P., Hirschberg, S. (2014) Comparative risk assessment of severe accidents in the energy sector. Energy Policy, 74, S45-S56.
- Burgherr, P., Spada, M. Kalinina, A., Hirschberg, S., Kim., W., Gasser, P. & Lustenberger, P. (2017) The Energy-related Severe Accident Database (ENSAD) for comparative risk assessment of accidents in the energy sector. IN: Cepin, M. & Bris, R. (Eds.) Safety and Reliability - Theory and Applications. London, UK, CRC Press, Taylor & Francis Group.
- Cinelli, M., Spada, M., Miebs, G., Kadziński, M., Burgherr, P. (2017, forthcoming) Classification models for the risk assessment of energy accidents in the natural gas sector. The 2nd International workshop on Modelling of Physical, Economic and Social Systems for Resilience Assessment. Brussels, Belgium.
- Hirschberg, S., Spiekerman, G., Dones, R. (1998) Severe accidents in the energy sector – 1st ed. PSI Report No. 98-16. Villigen PSI, Switzerland.
- Kalinina, A., Spada, M., Burgherr, P., Marelli, S. & Sudret, B. (2016) A Bayesian hierarchical modelling for hydropower risk assessment. IN: Walls, L., Revie, M. & Bedford, T. (Eds.) Risk, Reliability and Safety – Innovating Theory and Practice. London, UK, CRC Press, Taylor & Francis Group.
- Kim, W. Burgherr, P., Spada, M., Hirschberg, S., Lustenberger, P., Gasser, P. (2017) Transformation of the Energy-Related Severe Accident Database to an Open Source, Interactive, Web-Based GIS Application for Risk Visualization and Decision-Support. Free Open Source Software For Geospatial (FOSS4G) 2017, Boston, USA.
- Kyriakidis, M., Lustenberger, P., Burgherr, P., Dang, V. & Hirschberg, S. (2017) The human element in infrastructure resilience – a quantitative analysis of natural gas network recovery dynamics in floods. Proceedings of the PSAM Topical Conference on Human Reliability, Quantitative Human Factors, and Risk Management, Munich, Germany.

SCCER SoE
SWISS COMPETENCE CENTER for ENERGY RESEARCH
SUPPLY of ELECTRICITY

SCCER-SoE Annual Conference 2017

70 NRP Energy Turnaround
National Research Programme

In cooperation with the CTI
Energy
Swiss Competence Centers for Energy Research
Schweizerische Eidgenossenschaft
Confédération suisse
Confederazione Svizzera
Confederaziun svizra
Swiss Confederation
Commission for Technology and Innovation CTI

Probabilistic Damage Quantification of Unreinforced Masonry Walls Exposed to Induced Seismic Risk

Max Didier, Marco Broccardo, Giuseppe Abbiati, Fiona Hefti, Adrian Gabbi, Milos Petrovic, Nebojsa Mojsilovic, Bozidar Stojadinovic

Objective

Sequences of low-magnitude induced earthquakes can cause non-structural damage to buildings, for example, to the plaster covering the surface of unreinforced masonry (URM) walls. This construction style is prominent in Switzerland, as well as in other European countries. Deep geothermal reservoir exploration and operation can induce such seismic events. Two types of possible damage need to be distinguished: damage due to larger, more rare events; and damage due to fatigue caused by repeated, smaller events. An experimental test campaign has been led at the Institute of Structural Engineering (IBK) of ETH Zurich to quantify the probabilities of both types. The findings can be used in combination with an appropriate seismic hazard and ground motion model to quantify the (financial) risk of deep geothermal projects.

Test Campaign

In total, 15 plastered URM walls have been tested at ETH Zurich. The 5 walls of the first phase were tested using the NAMC and BIN2_99 load protocols, representative of low to medium magnitude seismicity. The 10 following walls were tested using a load protocol representative of fatigue loads. All walls were tested in a 3-actuator quasi-static test setup. Data on the reaction of the walls was collected using a laser sensor, several LVDT sensors and a digital image correlation (DIC) system. The pictures obtained via DIC were then processed in the Vic2D and Matlab software to obtain displacement and von Mises strain maps of the plaster surface. These maps were then used to compute damage scores to estimate the expected damage.

Damage Scores

Two damage scores have been developed and evaluated using the obtained experimental data: the Normalized Crack Area (NCA) and the Normalized Crack Length (NCL).

The **NCA** is defined as:

$$NCA = \frac{damaged\ area\ of\ the\ plaster}{total\ area\ of\ the\ plaster} = \frac{number\ of\ white\ pixels\ on\ cum.\ von\ Mises\ strain\ map}{total\ number\ of\ pixels\ on\ cum.\ von\ Mises\ strain\ map}$$

and the **NCL** as:

$$NCL = \frac{sum\ of\ length\ of\ all\ cracks}{length\ of\ wall\ diagonal} = \frac{sum\ of\ crack\ perimeters/2}{length\ of\ wall\ diagonal}$$

Both metrics are computed from the von Mises strain maps of the plaster surface (Fig. 1a)). The maps need to be converted first into greyscale maps (Fig. 1b)) to compute, finally, cumulate binary von Mises strain maps (Fig. 1c)). From these, the number of white pixels and the sum of the crack perimeters can be derived.

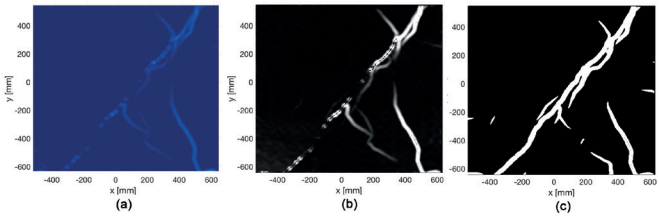

Fig. 1 a) von Mises strain map, b) greyscale von Mises strain map, and c) cumulate binary von Mises strain map

The computed damage scores can be correlated to the displacement amplitudes (Fig. 2). This allows to estimate the damage for a given displacement (e.g. imposed to the wall by an induced ground motion sequence at interest).

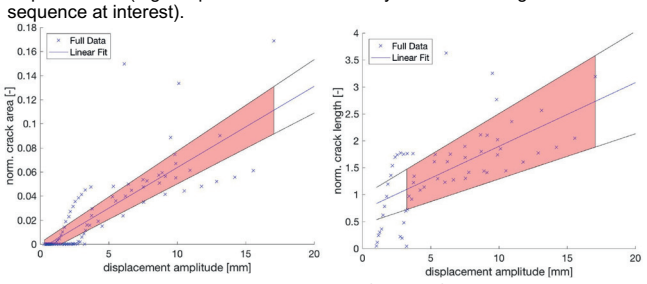

Fig. 2 Displacement amplitude and computed NCA and NCL

Damage States and Damage Probability

Three damage states have been defined to classify the damage of the walls:

- No damage: no visual damage detected on the picture;
- Visible crack: crack can be detected by visual inspection;
- Plaster fall-off: fall-off of parts of the plaster.

A survey has been conducted to correlate the calculated damage scores to the three damage states (Fig. 3). For a given NCA or NCL, the probability of observing a certain damage state can be estimated. In combination with Fig. 2, this allows to determine the probability of occurrence of damage to the plaster surface of an URM wall for a given displacement caused by an induced ground motion.

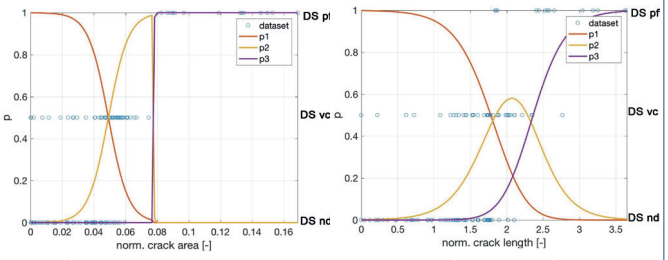

Fig. 3 Survey answers and multivariate logistic regression for NCA and NCL

Fatigue Damage

Experimental data obtained from applying fatigue-like load protocols on 10 walls was used to elaborate a fatigue damage model. Load sequences of amplitudes of 1mm, 3mm, 5mm and 7mm were applied up to 200 times to the same wall. The plaster surface was again analyzed by DIC. The NCA and the NCL were then computed for the progression of the fatigue tests (Fig. 4). An exponential regression was used to compute fatigue curves for plaster damage of the URM walls (Fig. 5).

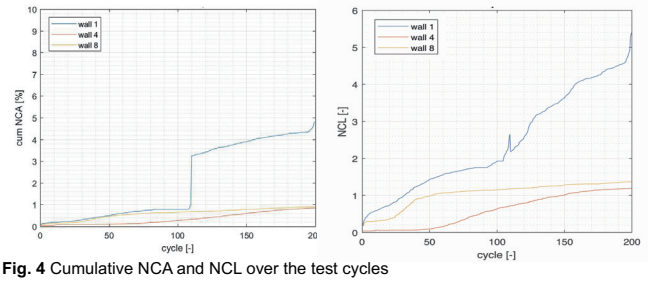

Fig. 4 Cumulative NCA and NCL over the test cycles

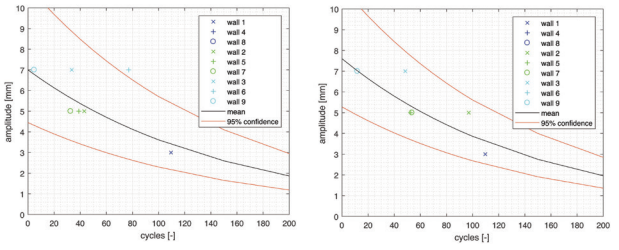

Fig. 5 Fatigue curves for NCA 1.0% and NCA 2.0%

Conclusion

Two damage scores have been developed using the data obtained from the experimental test campaign at ETH Zurich: the NCA, related to the damaged plaster surface; and the NCL, related to the length of the cracks on the plaster. Both metrics can be used to estimate the probability of observing a certain plaster damage state for a given displacement amplitude. The fatigue model allows to estimate the damage caused by long sequences of repeated induced ground motions. Combining the presented models with models for the expected induced seismicity of deep geothermal sites would allow to estimate the risk associated to such projects.

References

Didier, M., Abbiati, G., Broccardo, M., Beyer, K., Danciu, L., Petrovic, M., Mojsilovic, N., and Stojadinovic, B. (2017). Quantification of Non-Structural Damage in Unreinforced Masonry Walls Induced by Geothermal Reservoir Exploration using Quasi-Static Cyclic Tests. *Proceedings of 13th Canadian Masonry Symposium*, June 4-7, Halifax, Canada.

Mergos, P. E., & Beyer, K. (2014). Loading protocols for European regions of low to moderate seismicity. *Bulletin of Earthquake Engineering*, *12*(6), 2507-2530.

SCCER SoE
SWISS COMPETENCE CENTER for ENERGY RESEARCH
SUPPLY of ELECTRICITY

70 NRP Energy Turnaround
National Research Programme

ETH zürich

SCCER-SoE Annual Conference 2017

One decade of induced seismicity in Basel, Switzerland: A consistent high-resolution catalog obtained by template matching

Marcus Herrmann[1], Toni Kraft[1], Thessa Tormann[1], Luca Scarabello[1], Stefan Wiemer[1]

[1] Swiss Seismological Service, ETH Zürich, Switzerland; ✉ marcus.herrmann@sed.ethz.ch

In cooperation with the CTI
Energy
Swiss Competence Centers for Energy Research
Schweizerische Eidgenossenschaft
Confédération suisse
Confederazione Svizzera
Confederaziun svizra
Swiss Confederation
Commission for Technology and Innovation CTI
Schweizerischer Erdbebendienst
Service Sismologique Suisse
Servizio Sismico Svizzero
Swiss Seismological Service

Background & Problem Statement

In December 2006, an extensive fluid injection was carried out below the city of Basel, Switzerland, to stimulate a reservoir for an Enhanced Geothermal System (EGS).
Some details:

- ~11'500 m³ water injected into crystalline rock, 5km deep
- After 6 days, M_L2.6 event exceeded safety threshold
  → reduced injection rate, then stopped completely
  → shut-in (closure of borehole)
- Hours later: widely felt M_L3.4 event
  → well opened; rapid decay of seismicity
- Originally detected ~13'000 EQs (located ~3,500)
- Dec. 2009: project canceled – a seismic risk study suggested substantial risk of further felt and potentially damaging events [*Baisch 2009*]
- Mid-2011: ultimate shut-in; pressure increase
- Mid-2012: **renewed increase** of seismicity (M_L>1.0)

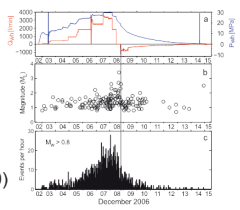

The well-monitored and well-studied induced sequence allowed many new insights in terms of reservoir creation. However, the **details of the long-term behavior** remained unexplored since a consistent catalog did not exist. We want to create one.

Highlights & Outlook

- Our newly obtained catalog …
  - spans more than ten years
  - contains **more than 130'000 events**
  - features a uniform detection threshold and consistent magnitude
  - decreased the detection limit by more than one magnitude unit
  - increased the spatiotemporal resolution
    → statistical analysis in great detail:
    - resolved variations of the a- and b-value
    - derived temporal development of the seismic hazard
    - …
- Detections confirm clearly the (re-)activity several years after injection; they tend to cluster
- Possible connection: pressure increase ↔ re-activation?
  - Since July 2017, the borehole is opened again periodically to reduce the pressure
  - ❑ How long do we have to monitor and maintain a closed EGS project?
- We hope to provide the basis for a better understanding of the processes that drive the induced seismicity in Basel
- We have also started to extend our analysis to other induced and natural sequences in Switzerland

Findings of a multi-template approach

We scanned the recordings of the **deepest installed borehole station** (2.7km). This station is very close (1.5–2.5km) to ~4.5km-deep reservoir, completely in the granite bedrock. It has the highest signal-to-noise ratio among all (borehole-)stations.

Technical details:
- Band-pass-filter of 5-80Hz; 500fps
- Removed 50Hz noise in the frequency domain
- The Z-channel failed in 2010. To be consistent, we only used the 2 horizontal channels. This might lead to wrong template associations.

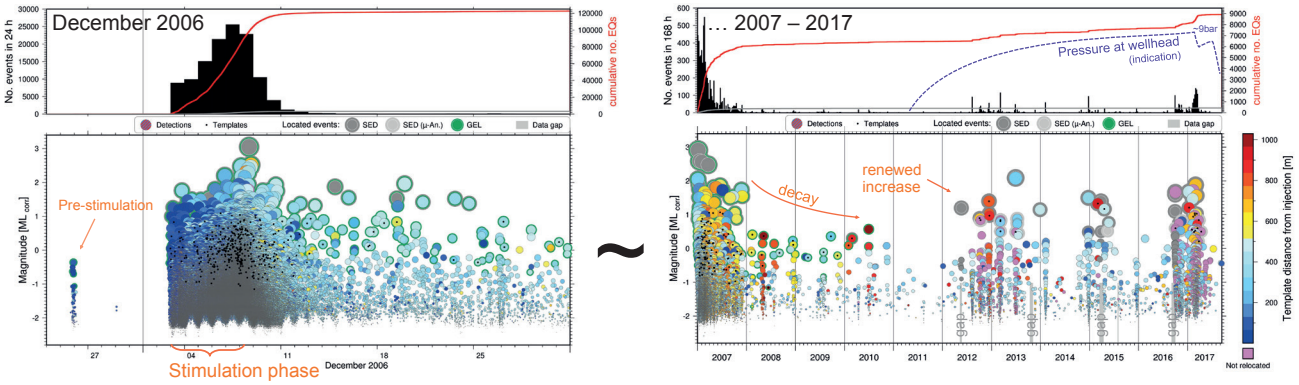

The color of a detection indicates to which template it is most similar. Later events tend to occur and cluster more outwards. But also older (inner) fault patches get reactivated again.

The orientation of the individual faults varies and deviates from the general orientation "seismic cloud" [*Deichmann et al. 2014*]. To reach an acceptable coverage of the complex seismicity in the stimulated volume, we selected **~500 templates** from >3'600 event waveforms and performed the scan in **parallel on ~600 cores** of the EULER high-performance computer. This scan over more than 10 years of data took ~36 hours.

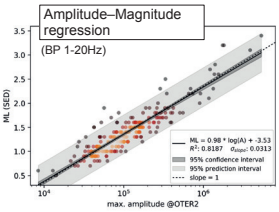

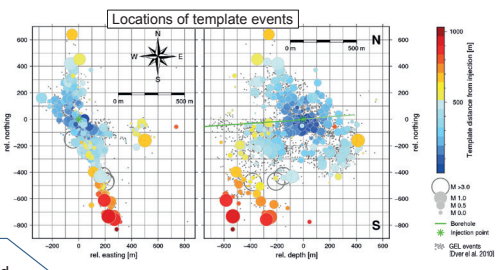

Earthquake statistics

The sampling of the seismic sequence in much closer detail significantly improved the completeness magnitude (*Mc*) of the catalog so that we can **resolve the *b*-value variation** and **thus the probability for a larger event** in unprecedented resolution. In particular, we can now assess the long-term evolution of the sequence even during periods when the rate of network-detected events is very low (e.g., 2010 – 2011).

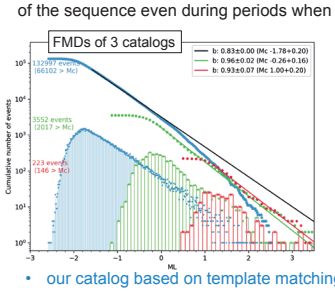

- our catalog based on template matching
- *Dyer et al. 2010*
- *Swiss Seismological Service (SED)*

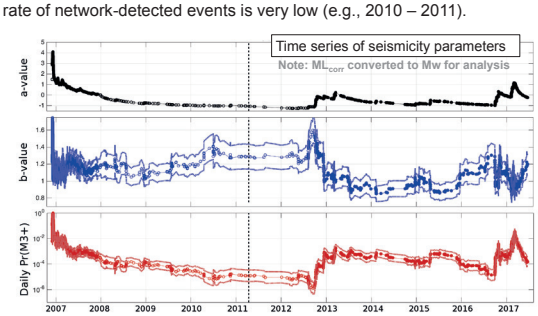

Acknowledgements

We thank *GeoEnergie Swiss AG* and *GeoExplorers Ltd.* for providing the seismometer recordings of the Basel Geothermal Project. A special thanks goes to the team of the EULER high-performance computer (Swiss National Supercomputing Centre) for providing us plenty of computational power.
This work was conducted with the support of ENERGIESCHWEIZ in the framework of the project GEOBEST-CH. The research leading to these results has also received funding from the *European Community's Seventh Framework Programme* under grant agreement No. 608553 (Project *IMAGE*).

References

Baisch, S., Carbon, D., Dannwolf, U. S., Delacou, B., Devaux, M., Dunand, F., … Vörös, R. (2009). Deep Heat Mining Basel: Seismic Risk Analysis.

Dyer, B.C., et al., 2010. Application of microseismic multiplet analysis to the Basel geothermal reservoir stimulation events. Geophys. Prospect. 58.

Deichmann, et al., 2014. Identification of faults activated during the stimulation of the Basel geothermal project from cluster analysis and fault mechanisms for the larger magnitude events. Geothermics.

SCCER SoE
SWISS COMPETENCE CENTER for ENERGY RESEARCH
SUPPLY of ELECTRICITY

ETH zürich

SCCER-SoE Annual Conference 2017

Generic cellular automaton for statistical analysis of landslides frequency-size distribution

Ahoura Jafarimanesh, Arnaud Mignan, and Domenico Giardini

In cooperation with the CTI
Energy
Swiss Competence Centers for Energy Research
Schweizerische Eidgenossenschaft
Confédération suisse
Confederazione Svizzera
Confederaziun svizra
Swiss Confederation
Commission for Technology and Innovation CTI
70 NRP Energy Turnaround
National Research Programme

Abstract:

This study presents a generic landslide cellular automaton (GLSCA) that is constructed based upon the rules of Self Organized Criticality (SOC) and is consistent with the broad range of values in nature. Despite different triggering mechanisms in landslides processes (e.g., rain, earthquakes, etc.), the related frequency-size distribution (FSD) appears to follow the power law probability function, with the power law exponent (α) valid for x ≥ xmin. Here, we study the role of various triggering mechanisms in addition to the soil characterization on α. The landslide activation is based on the factor of safety (FS), (e.g., Crosta, 1998 and references therein), and the dynamic of the model is controlled by the ground slope variation. We attempted to interpret the physical behaviour of the landslide (e.g., exponential roll over effect) based on α variation, and test other metrics such as the maximum extent per earthquake magnitude and landslide shape. In that, we demonstrated how our GLSCA compares to studies that have reported frequency distributions of landslides areas in the world.

Power law function and probability distributions:

Power law probability density function with the exponent (α) valid for $x \geq x_{min}$

(1) $$p(x)=(\alpha-1)x_{min}^{\alpha-1}\,x^{-\alpha}$$

To study the roll over behaviour below x_{min}, double pareto (2) and inverse gama distribution (3) have been proposed:

(2) $$p(x)=\frac{\beta}{x_c}\left[\frac{(1+(\max x/x_c)^{-\alpha_2})^{\beta/\alpha_2}}{(1+(x/x_c)^{-\alpha_2})^{1+\beta/\alpha_2}}\right]\left(\frac{x}{x_c}\right)^{-\alpha_2-1}$$

(3) $$p(x)=\frac{1}{x_c\Gamma(\rho)}\left(\frac{x_c}{x-s}\right)^{\rho+1}\exp\left(-\frac{x_c}{x-s}\right)$$

Parameters (1) : **α** = **α**$_2$+1 ,**β** the power exponent below the rollover , $\boldsymbol{x_c}$ the corner size; Parameters (2) : **α** =**ρ+1**, ***s*** a parameter primarily controlling the exponential rollover, and $\boldsymbol{x_c}$ the corner size.

Landslide frequency size statistic and sampling:

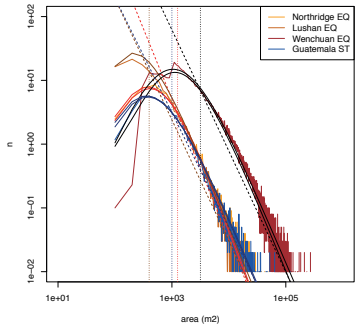

Fig. 1: The FSD of published landslide inventories. The power law exponent α ,(Eq. 1) for each case is equal to :

1:1994 Northridge earthquake (Harp and Jibson, 1995), α_1=2.4
2: 2013 Lushan earthquake (Xu et al., 2015), α_2=3
3: 2008 Wenchuan earthquake (Li et al., 2014), α_3=3
4: 1998 Hurricane Mitch (Bucknam et al., 2001) , α_4= 2.2

Updated table of α value correspondent to 50 landslide inventories shows α distribution with 2<α< 3 (Jafarimanesh et al., 2017- in preparation)

Generic Landslide Cellular Automaton (GLSCA):

A. Initiation phase: Landslide initiate when the factor of safety (Fs) is ≤ 1.

(4) $$FS=\frac{C}{\gamma h\sin\theta}+\frac{\tan\phi}{\tan\theta}-\frac{m\gamma_w\tan\phi}{\gamma\tan\theta}$$ (Jibson,1993) Earthquake triggered

(5) $$FS=\frac{\tan\phi}{\tan\theta}-\frac{-\Psi(Z,t)\gamma_w\tan\phi}{\gamma_w Z\sin\theta\cos\theta}+\frac{C}{\gamma_s Z\sin\theta\cos\theta}$$ (Iverson,2000) Rainfall triggered

Φ the effective internal friction angle, C the soil cohesion ,θ the slope angle, γ the soil unit weight, γ_w the water unit weight, h the slope-normal soil thickness, m the proportion of h that is saturated, γ_s is the depth-averaged soil unit weight, and ψ(Z,t) is the pressure head which determines the effect of the groundwater on slope stability.

B. **Propagation phase:** Altitude *z*(x,y) and soil depth *h*(x,y).

(6) $$\begin{cases} z(x,y)=z(x,y)-\Delta h \\ h(x,y)=h(x,y)-\Delta h \\ z(dir_{Moore}[\theta_{max}(x,y)])=z(dir_{Moore}[\theta_{max}(x,y)])+\Delta h \\ h(dir_{Moore}[\theta_{max}(x,y)])=h(dir_{Moore}[\theta_{max}(x,y)])+\Delta h \end{cases}$$

Input parameters are the initial topography (*z*, *h*) and soil properties (ϕ, *C*, Υ, *m)*

and the mass movement is defined by Eq. 7:

(7) $$\Delta h=[z(x,y)-z(dir_{Moore}[\theta_{max}(x,y)])-\Delta s\tan(\theta_{stable})]/2$$

Algorithm, fractal topography modelling and the GLSCA application:

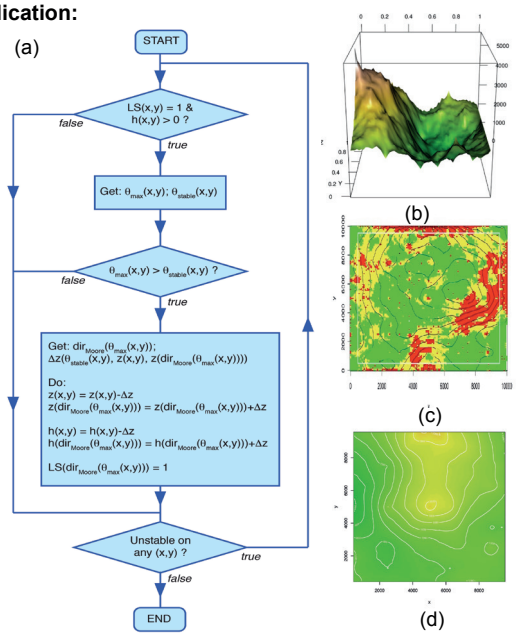

Fig. 2 : (a) Algorithm of the proposed CA method. (b): The example of fractal topography used in the modelling. (c) The factor of safety map, red cells are showing Fs<1 and yellow cells indicate 1≤Fs≤1.5 . (d) The new eroded topography after the analysis, the critical cells are removed.

Results :

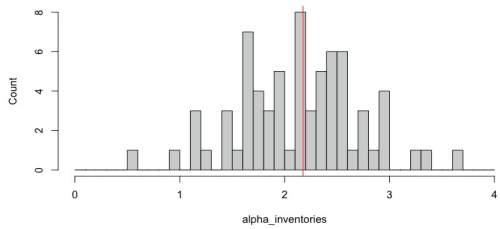

Fig. 3: The histogram of α values, correspondent to 50 frequency distribution of landslide areas worldwide (updated from Van Den Eeckhaut et al., 2007). The vertical red line shows the median of α values is around 2.1.

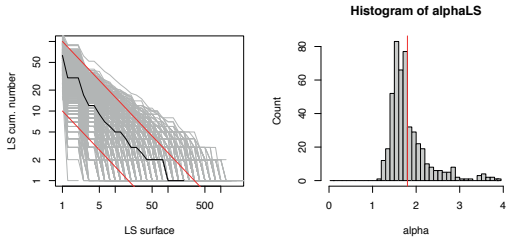

Fig. 4: (a) The FSD of CA method applied over 500 cases of fractal topographies. The Inclined red lines show the boundary of the analysis. (b) The histogram of non cumulated α values of analysis in (a); The vertical red line shows the median of the α values is approximately around 1.9.

Reference (Database):

- Van Den Eeckhaut, Miet, et al. "Characteristics of the size distribution of recent and historical landslides in a populated hilly region." Earth and Planetary Science Letters 256.3 (2007): 588-603.

SCCER SoE
SWISS COMPETENCE CENTER for ENERGY RESEARCH
SUPPLY of ELECTRICITY

SCCER-SoE Annual Conference 2017

70 NRP Energy Turnaround
National Research Programme

PAUL SCHERRER INSTITUT PSI

In cooperation with the CTI
Energy
Swiss Competence Centers for Energy Research
Schweizerische Eidgenossenschaft
Confédération suisse
Confederazione Svizzera
Confederaziun svizra
Swiss Confederation
Commission for Technology and Innovation CTI

Uncertainty quantification of flood wave propagation resulting from a concrete dam break

Anna Kalinina[1], Matteo Spada[1], Peter Burgherr[1], & Christopher T. Robinson[2]

[1]Technology Assessment Group, Paul Scherrer Institut, Villigen, Switzerland, [2] Department of Aquatic Ecology, Eawag, Dübendorf, Switzerland

Research scope and goal definition

Modelling of the dam-break event consists of 3 simulation Blocks:

Block 1: Dam-break outflow hydrograph → Block 2: Dam-break flood simulation → Block 3: Estimation of loss of life

Research scope: In the current phase of the PhD project, we focus on the model that evaluates the flow quantities reached downstream of the dam in case of a failure (**Block 1** and **Block 2**)

Research goals: **Metamodelling for uncertainty quantification and sensitivity analysis** is applied in the model of a large concrete dam break; Developing a generic model that can be used for analysis of any dam in Switzerland.

Generic physical model of flood wave propagation resulting from a concrete dam break

- The focus of the model is on large arch concrete hydropower dams located in the Alpine area of Switzerland;
- Complete and instantaneous failure of the dam is assumed; therefore, the dam-break is treated as a Riemann problem;
- The amount of water released from the dam is characterized using **4** parameters: *H, C, V, B_{rel}* (**Table 1**);
- Flood propagation is simulated for a generic model of the downstream valley characterized using **6** parameters: *CL_{rel}, CW_{rel}, shCH, BS, Mb*, & *Ms* (**Table 1**);
- A 1D model is then built in the BASEMENT software (ETHZ).

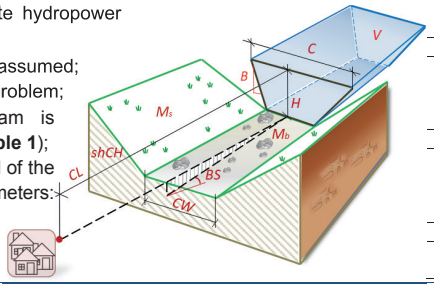

Table 1: Model Input Parameters

Par-r	Name	Unit
Physical characteristics of dam and reservoir		
H	Dam height	[m]
C	Length of dam crest	[m]
V	Reservoir volume	[10^3*m^3]
B_{rel}	Dam side slope (relative)	[m/m]
Physical characteristics of channel		
CL_{rel}	Channel length (relative)	[m/m]
CW_{rel}	Channel bed width	[m]
shCH	Shape parameter of channel cross section	[m^3]
BS	Slope of channel bed (relative)	[%/m]
Environmental characteristics		
Mb	Roughness coefficient of channel bed	[sec/$m^{1/3}$]
Ms	Rough. coeff. of channel embankments	[sec/$m^{1/3}$]

Framework for uncertainty quantification & sensitivity analysis

Modeled input uncertainty is propagated through the surrogate model created using **Polynomial Chaos Expansion (PCE)**:

$$Q_{peak} = \sum_{\alpha \epsilon A} y_\alpha \Psi_\alpha(X)$$

Q_{peak} - PCE response, X_i - input vector, y_α - coefficient, Ψ_α - polynomials

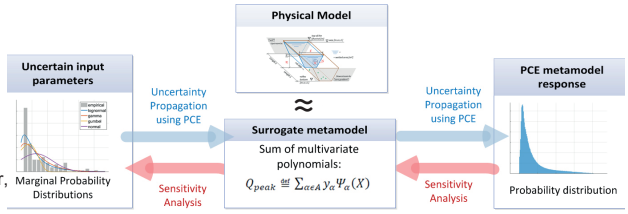

Sensitivity Analysis is performed using the linear correlation coefficient ρ_i between the i^{th} input and the model output Q_{peak}; and the Spearman rank correlation coefficient ρ_i^S.

Building a metamodel and sensitivity analysis are performed using UQLab (Marelli and Sudret, 2014).

Results for uncertainty & sensitivity of the model parameters

Model input uncertainty:

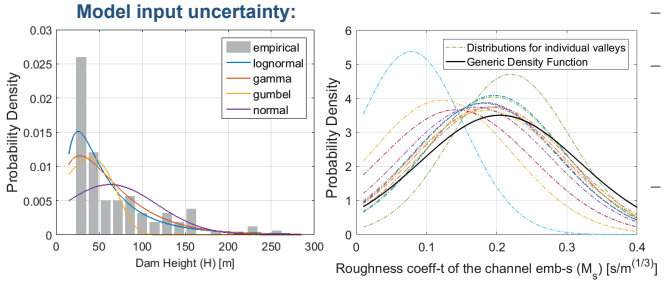

Model output uncertainty and sensitivity:

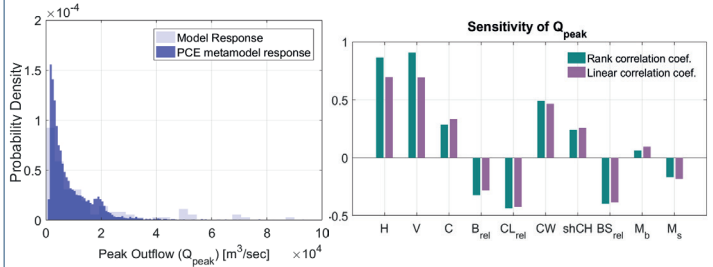

- Distributions of **4** input parameters (*H, C, V, B_{rel}*) are built using the data of 116 large dams in Switzerland (SwissCOD, 2016);
- Distributions of **6** other input parameters (*CL_{rel}, CW_{rel}, shCH, BS, Mb*, & *Ms*) are defined by classifying topographies downstream of 19 arch concrete dams in Switzerland. The classification is based on slopes and land cover data from GeoVITE (https://geodata4edu.ethz.ch/portal.jsp) & Rosgen, et al. (2013);
- Dependence between parameters was modelled by a Gaussian copula; certain distributions are truncated due to physical constrains.

Table 2: Marginal distributions of model inputs

Par-r	Distribution	Par-r	Distribution
H	$H \sim LN(3.83, 0.77)$	CW_{rel}	$CW_{rel} \sim \Gamma(0.013, 0.58)$
V	$V \sim LN(8.04, 2.76)$	shCH	$shCH \sim \Gamma(1.4e-4, 13.6)$
C	$C \sim \Gamma(0.007, 1.6)$	BS	$BS \sim LN(2.44, 0.57)$
B_{rel}	$B_{rel} \sim U(0, 1)$	Mb	$Mb \sim LN(-2.63, 0.95)$
CL_{rel}	$CL_{rel} \sim \Gamma(0.04, 2.22)$	Ms	$Ms \sim N(0.20, 0.11)$

- **PCE** is calculated for the set of **flow quantities** at the location downstream of the dam, i.e., peak discharge Q_{peak} [m^3/sec], the time to the Q_{peak} [sec], and water depth [m];
- **PCE** is built using a design sample of **111 runs** of the **original model**;
- The dam dimensions, channel bed width and its slope are **important** for the Qpeak; as well as it is important how far from the dam the inhabited locality, where the flow quantity need to be measured, is situated.

Conclusions:
- The applied metamodelling approach can reproduce the original model, and allows **reducing computational efforts**.
- Sensitivity analysis can **support decision-making processes**, thus being **beneficial for the risk assessment field**.
- The generic model can be used for **analysis of any existing dam in Switzerland**, as well as dams **currently in design**.

Acknowledgement: This research project is part of the National Research Programme "Energy Turnaround" (NRP 70) of the Swiss National Science Foundation (SNSF). Further information on the National Research Programme can be found at www.nrp70.ch. It is also integrated with the activities of the Swiss Competence Center on Energy Research – Supply of Electricity (SCCER SoE).

The authors express their sincere thanks to Prof. Bruno Sudret and Dr. Stefano Marelli, ETHZ, and to Dr. David Vetsch, ETHZ, for valuable comments and assistance.

References
- Rosgen, et al. (2013). Waldo Canyon Fire Watershed Assessment: The WARSSS Results. Wildland Hydrology, 4 Appendices.
- ETH Zurich 2016. BASEMENT, Accessed in: http://www.basement.ethz.ch/.
- Marelli, S. & Sudret, B. 2014. UQLab: A framework for uncertainty quantification in Matlab 257 Vulnerability, Uncertainty, and Risk. 2nd ICVRAM2014, UK.
- SwissCOD 2016. Dams in Switzerland, Accessed in: http://www.swissdams.ch/index.php/en/swiss-dams/dams-in-switzerland.

SCCER SoE
SWISS COMPETENCE CENTER for ENERGY RESEARCH
SUPPLY of ELECTRICITY

SCCER-SoE Annual Conference 2017

FNSNF
SWISS NATIONAL SCIENCE FOUNDATION

Communicating induced seismicity of deep geothermal energy and shale gas: low-probability high-consequence events and uncertainty[1]

Theresa Knoblauch, Michael Stauffacher, Evelina Trutnevyte
ETH Zurich, Department of Environmental Systems Science (USYS), USYS Transdisciplinarity Lab

1 Motivation

- Deep geothermal energy (DGE) guidelines [2,3] recommend to communicate low-probability high-consequence (LPHC) events of induced seismicity (IS) to the public.
- However, risk communication literature lacks empirical evidence on how to communicate LPHC events of IS and whether to address related uncertainty.

2 Research questions

1) How do **different formats** of written risk communication of IS affect the public's perception of this risk communication in terms of **understandability, trust, and concern**? We distinguish between three formats (qualitative, qualitative and quantitative, qualitative and quantitative with risk comparisons).

2) How does **a statement of uncertainty and limited expert confidence** affect the public's perception of this risk communication in terms of understandability, trust, and concern?

3) How does the risk communication format affect the **public's perception of the risk** of IS?

4) To what extent does the technology, such as DGE and shale gas, affect the public's perception of the identical risk communication material?

3 Method

- Online survey August 2016
- Experimental design
- N = 590 participants
- German-speaking part of Switzerland

Table I Experimental conditions (C) of the survey

Format	Statement of uncertainty	Technology	
		DGE	Shale gas
Qualitative	Not included	C1	C7
	Included	C2	C8
Quantitative	Not included	C3	C9
	Included	C4	C10
Risk comparison	Not included	C5	C11
	Included	C6	C12

4 Technology framing

Figure 1 Detail of technology framing
Left: Near surface and deep geothermal energy [4,5]
Right: Conventional gas and shale gas with hydraulic fracturing[6,7]

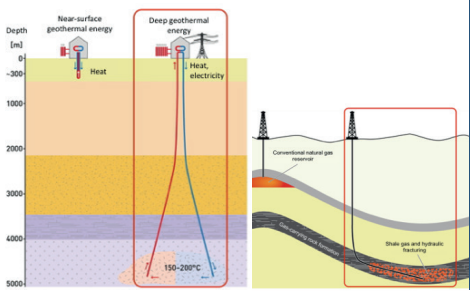

5 Risk communication for experimental conditions

Table II Examples of risk communication formats for different experimental conditions (C)

Qualitative format (C1, C7)

The risk study concluded for the week-long drilling and project operations in your community:
- Micro-earthquakes are virtually certain. These micro-earthquakes will be too small for humans to be felt.
- An earthquake that is lightly noticeable for humans is unlikely.
- An earthquake that is strongly felt and can cause slight damage (e.g. hair-line cracks or falling of small pieces of plaster) is exceptionally unlikely.
- An earthquake that is severely felt and can cause serious structural damage to average houses (e.g. large cracks in walls, falling of gable parts) is even more unlikely, thus also exceptionally unlikely.

Quantitative format with uncertainty and limited expert confidence (C4, C10)

The risk study concluded for the week-long drilling and project operations in your community:
- Micro-earthquakes are virtually certain. These micro-earthquakes will be too small for humans to be felt.
- An earthquake of magnitude 3 on the Richter scale that is lightly noticeable for humans has a probability of about 5%.
- An earthquake of magnitude 5 on the Richter scale that is strongly felt and can cause slight damage (e.g. hair-line cracks or falling of small pieces of plaster) is exceptionally unlikely. It has a probability of about 0.01%.
- An earthquake of magnitude 6 on the Richter scale that is severely felt and can cause serious structural damage to average houses (e.g. large cracks in walls, falling of gable parts) is even more unlikely, thus also exceptionally unlikely. It has a probability of about 0.001%.

The risk assessment is based on best available methods. Due to unpredictable reactions in the subsoil, such risk assessments carry uncertainty. Therefore, experts can disagree on the exact probabilities and the largest possible earthquake.

6 Main results

Figures II-IV: $\bar{x}$: grand mean; significance level *p<0.05; ** p<0.01; ***p<0.001 for difference between conditions
Ratings range from 1= "do not agree at all" to 7= "completely agree". "Don't know" option coded as missing value.

1) Risk communication format
Figure II: Perception of different risk communication formats between conditions

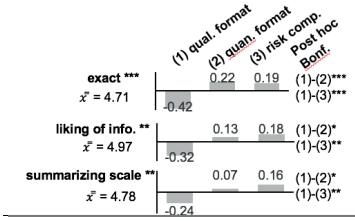

2) Including statement of uncertainty and expert confidence
Figure III: Effect of including a statement of uncertainty and expert confidence between conditions

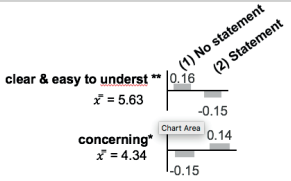

3) Perceived risk

- The format had no effect on respondents' risk perception of IS.
- The risk of IS seemed significantly less controllable when respondents read statement about uncertainty as compared to not reading about it (M 3.47, SD = 1.52 vs. M = 3.72, SD = 1.47), F(1,568)=3.91, p=0.048.
- Respondents perceived the risk of IS significantly higher for shale gas than for DGE (M = 4.81, SD = 1.13 vs. M = 4.19, SD = 1.14), F(1,589) = 43.83, p<0.001.

4) Technology framing
Figure IV: Effect of technology framing between conditions

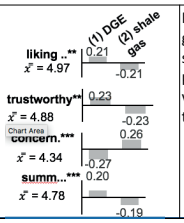

Respondents accepted shale gas projects in their region significantly less than DGE projects (M = 3.47, SD = 1.70 vs. M = 5.02, SD = 1.36), t(481)=11.41, p<0.001.

7 Conclusions

- Respondents perceived the quantitative and risk comparison format more exact and liked it more. They also found it easier to understand (n.s.).
- Respondents perceived risk communication including uncertainty and expert confidence as less clear and more concerning.
- Respondents perceived identical risk communication for shale gas as less trustworthy, more concerning and liked it less than for DGE.
- **Recommendation for practitioners:**

→The public appreciates careful elaboration of risk communication with numbers and suitable risk comparisons.

→The public might have difficulties in understanding information about uncertainty.

→Besides the careful wording of risk communication, the context matters!

References

[1] Knoblauch T., Stauffacher M., Trutnevyte E. (2017). Communicating low-probability high-consequence risk, uncertainty and expert confidence: Induced seismicity of deep geothermal energy and shale gas. Risk Analysis. Under review.
[2] Trutnevyte, E., & Wiemer, S. (2017). Tailor-made risk governance for induced seismicity of geothermal energy projects. *Geothermics*, *65*, 295–312.
[3] Majer, E. L., Nelson, J., Robertson-Tait, A., Savy, J., & Wong, I. (2012). *Protocol for addressing induced seismicity associated with enhanced geothermal systems. Geothermal Technologies Program*. U.S. Department of Energy.
[4] Department für Inneres und Volkswirtschaft Kanton Thurgau [Department for internal affairs and political economicy canton Thurgau]. (2009). Geothermie – die nachhaltige Energiequelle [Geothermal energy - the sustainable energy resource]. Retrieved April 4, 2016, from www.energie.tg.ch
[5] KBB Underground Technologies. (2016). Geothermie: Zuverlässige Energie aus den Tiefen unserer Erde [Geothermal energy: Reliable energy from our Earth's depths]. Retrieved April 4, 2016, from http://www.kbbnet.de/fachbereiche/geothermie/
[6] Europäisches Institut für Klima und Energie [European Institute for climate and energy]. (2010). Schiefergas als alternativer Energierohstoff – nur eine goldrauschähnliche Euphorie? [Shale gas as alternative resource - only a gold-rush-like euphoria]. Retrieved April 4, 2016, from http://www.eike-klima-energie.eu/climategate-anzeige/schiefergas-als-alternativer-energierohstoff-nur-eine-goldrauschaehnliche-euphorie/
[7] Bundesanstalt für Geowissenschaften und Rohstoffe [Federal Office for geoscience and resources]. (2016). Schieferöl und Schiefergas in Deutschland [Shale oil and shale gas in Germany].

SCCER SoE
SWISS COMPETENCE CENTER for ENERGY RESEARCH
SUPPLY of ELECTRICITY

SCCER-SoE Annual Conference 2017

SWISS NATIONAL SCIENCE FOUNDATION

Where to site Enhanced Geothermal Systems (EGS)? Trading off heat benefits and induced seismicity risk from the investor's and society's perspective

Theresa Knoblauch, Evelina Trutnevyte
ETH Zurich, Department of Environmental Systems Science (USYS), USYS Transdisciplinarity Lab

Introduction

There is a dilemma when siting EGS projects as siting influences both induced seismicity (IS) risk of EGS projects as well as their profitability [1,2].

On the one hand, when siting EGS in remote areas, building exposure and thus IS risk is reduced [3,4,5].

On the other hand, when siting EGS close to buildings, heat can be purposefully used by supplying it to a dense district heating network (DHN). This reduces costs of EGS projects and avoids CO_2 emissions by heat systems [6,7].

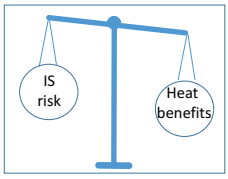

Figure 1 Trading off risk of IS and heat benefits when siting EGS.

Method

We use cost benefit analysis (CBA) to quantify this trade-off of siting EGS of different capacities in remote or in densely populated areas. We analyze 16 hypothetical scenarios that are combinations of different EGS and siting (Table 1).

We model the EGS plant and its heat and electricity production in detail and couple it to a stylized model of IS hazard and risk which is sufficient for CBA given high uncertainties and lack of data for IS [8].We distinguish between CBA from investor's and society's perspective [9]. CBA from investor's perspective includes Net Present Value (private) and Internal Rate of Return (IRR) as well as Levelized Cost of Electricity (LCOE) of the EGS in every scenario. CBA from society's perspective reflects costs and benefits to the society as a whole. In addition to direct costs and revenues, also damage due to IS and CO_2 savings with respect to conventional electricity and heat production are included to quantify NPV (social) and Benefit-to-Cost ratio (B/C ratio).

		Circulation rate [l/S]			
		50	**100**	**150**	**200**
Residents	**0**	S 1	S 2	S 3	S 4
	1'000	S 5	S 6	S 7	S 8
	10'000	S 9	S 10	S 11	S 12
	100'000	S 13	S 14	S 15	S 16

Table 1 EGS scenarios.

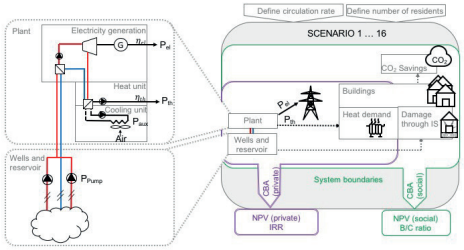

Figure 2 EGS framework for CBA from investors and society's perspectives.

Results of CBA from investor's perspective

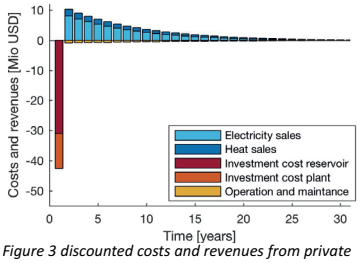

Figure 3 discounted costs and revenues from private perspective illustrated for EGS scenario 11.

Figure 3 shows direct costs and revenues, exemplarily depicted for EGS scenario 11 (150 l/s circulation rate, 10'000 residents). EGS come with high upfront investment costs followed by decreasing revenues from electricity during lifetime as EGS reservoir temperature declines due to thermal drawdown.

According to Figures 4 and 5, EGS are most profitable from investor's perspective when sited surrounded by large number of residents (10'000 or 100'000) and when operated with high circulation rate (150 l/s or 200 l/s).

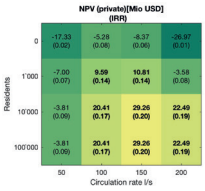

Figure 4 NPV (private) and IRR for EGS scenarios.

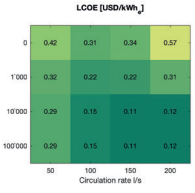

Figure 5 LCOE for EGS scenarios.

Results of CBA from society's perspective

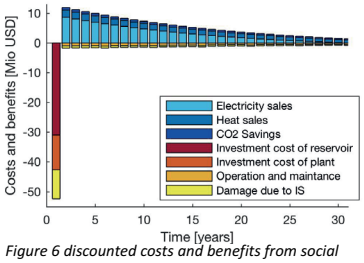

Figure 6 discounted costs and benefits from social perspective illustrated for EGS scenario 11.

Figure 6 presents direct and indirect costs and benefits for the wider society, exemplarily depicted for EGS scenario 11 (150 l/s circulation rate, 10'000 residents). Damage due to IS amounts to significant costs when creating the reservoir, whereas benefits of CO_2 savings are rather negligible.

According to Figures 7 and 8, EGS are most profitable from social perspective when sited surrounded by some residents (1 '000 or 10 '000) and when operated with medium circulation rate (100 l/s or 150 l/s).

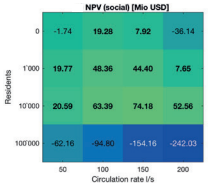

Figure 7 NPV (social) for EGS scenarios.

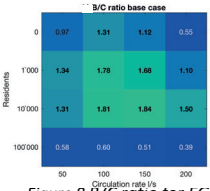

Figure 8 B/C ratio for EGS scenarios (base case).

Conclusions

- Results of CBA from investor's perspective suggest to preferably site EGS in areas where all remaining heat can be sold to a DHN, thus towns or cities with surrounding number of residents equal or larger than 10'000. In contrast, results of CBA from society's perspective suggest to site EGS where a fair amount of remaining heat can be sold but at the same time damage due to IS is limited, thus 1'000 or 10'000 surrounding residents. When considered jointly, CBA from both, investor's and society's perspectives suggests that EGS in remote areas are not as profitable as siting EGS surrounded by at least some residents due to lacking revenues from heat.

- CBA from both investor's and society's perspective suggests to implement an EGS of a certain circulation rate respecting two constraints: one, a minimum constraint of circulation rate ensures that EGS produces sufficient electricity and heat in order to compensate and ideally exceed high upfront investment costs. Two, a maximum constraint of circulation rate should ensure that pump power does not exceed net electricity output of EGS and thus prevents additional electricity supply from grid which would considerably decrease profitability. Plus, according to our model, damage due to IS also increases with circulation rate.

References

[1] T. Kraft, P. M. Mai, S. Wiemer, N. Deichmann, J. Ripperger, P. Kästli, C. Bachmann, D. Fäh, J. Wössner, and D. Giardini, "Enhanced Geothermal Systems: Mitigating Risk in Urban Areas," *Eos, Trans. Am. Geophys. Union*, vol. 90, no. 32, pp. 273–274, 2009.
[2] W. Schenler, "Economy," in *Energy from the Earth: Deep Geothermal as a Resource for the Future? TA Swiss Geothermal Project Final Report.*, S. Hirschberg, S. Wiemer, and P. Burgherr, Eds. Villingen, Switzerland: Paul Scherer Institute, 2015, pp. 155–182.
[3] E. L. Majer, R. Baria, M. Stark, S. Oates, J. Bommer, B. Smith, and H. Asanuma, "Induced seismicity associated with Enhanced Geothermal Systems," *Geothermics*, vol. 36, no. 3, pp. 185–222, 2007.
[4] J. J. Bommer, H. Crowley, and R. Pinho, "A risk-mitigation approach to the management of induced seismicity," *J. Seismol.*, vol. 19, no. 2, pp. 623–646, 2015.
[5] A. McGarr, B. Bekins, N. Burkhardt, J. Dewey, P. Earle, W. Ellsworth, S. Ge, S. Hickman, A. Holland, E. Majer, J. Rubinstein, and A. Sheehan, "Coping with earthquakes induced by fluid injection: Hazard may be reduced by managing injection activities," *Science.*, vol. 347, no. 6224, pp. 830–831, 2015.
[6] Department of Energy & Climate Change (DECC), "Deep geothermal review study. Final report," 2013.
[7] M. Beerepoot, "Technology roadmap - geothermal heat and power," 2011.
[8] E. Trutnevyte and I. L. Azevedo, "Expert agreements and disagreements on induced seismicity by Enhanced Geothermal Systems," *Manuscr. Submitt. Publ.*
[9] K. Blok and E. Nieuwlaar, "Economic analysis of energy technologies," in *Introduction to energy analysis*, Second edi., E. Nieuwlaar, Ed. London, New York : Routledge, Taylor & Francis Group, earthscan from Routledge, 2017, p. xxv, 310 pages

SCCER SoE
SWISS COMPETENCE CENTER for ENERGY RESEARCH
SUPPLY of ELECTRICITY

SCCER-SoE Annual Conference 2017

In cooperation with the CTI
Energy
Swiss Competence Centers for Energy Research
Schweizerische Eidgenossenschaft
Confédération suisse
Confederazione Svizzera
Confederaziun svizra
Swiss Confederation
Commission for Technology and Innovation CTI

The price of public safety in EGS projects

A. Mignan, M. Broccardo, S. Wiemer & D. Giardini

Abstract

The risk associated with seismicity caused by fluid injection in the deep underground in EGS projects can be faced using mitigation measures, such as traffic light systems (TLS), which impose a risk threshold criterion in order to ensure public safety. This infers that some wells may fail, which would tend to increase the EGS-generated electricity base price. We first estimate this increase as a function of borehole distance *d* to the nearest habitation considering a probability of fatality higher than 10^{-6} as unacceptable. Taking into account the underground feedback uncertainty (*a*- and *b*-values of the Gutenberg Richter law, maximum magnitude M_{max}), standard risk parameters and a reasonable economic model (base price of 0.20$/kWh), we find that the price increases to 0.23$/kWh above the borehole and rapidly decreases back to the base price at a distance *d* = 40km. Based on Cumulative Prospect Theory, we find the price to increase to 0.30$/kWh due to the risk aversion of uncertain well loss. The heat credit at short distances would compensate for this "cost of public safety" – *Disclaimer: All values are subject to modelling choices.*

Methods

- Project: triplet, depth z = 5km, stimulation of V = 30,000m^3
- Electricity generation (e.g., *Lacirignola & Blanc*, 2013): T_{prod} = 35z °C, T_{reinj} = 70°C, Q = 50l/s, ORC system (case 5), 8000hr/yr, P_{net} ≈ 2MW, E_{net} ≈ 15 GWh/yr, plant/well life of 20yr
- Costs (*Hirschberg et al.*, 2015): C_{well} = 20 million $, C_{frac} = 1 million $, C_{plant} = 4000$/kW
- Pricing = costs ($) / electricity generation (kWh) = **0.20 $/kWh**
- Induced seismicity risk model (*Mignan et al.*, 2015): RISK-UE method, intensity prediction equation, EMS98 class B building
- Risk mitigation TLS-based model (*Mignan et al.*, in rev.): p = **probability of fatality** curve crossing the **10^{-6} safety threshold**
- Price updating approach: additional cost per failed well = $p(C_{well}+C_{frac})$
- Risk aversion model: standard parameters of Cumulative Prospect Theory CPT (*Tversky & Kahneman*, 1992) with distortion of p, loss aversion amplification & different utility functions for losses/gains

Results

- Underground feedback uncertainty: M_{max} ambiguity turned into subjective probability (Pr(M_{max}=4)=Pr(M_{max}=7)=0.5); Worldwide (*a*, *b*) scattering assumed as true distribution & independent of well location

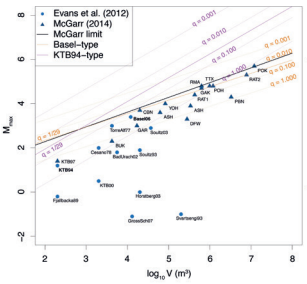

McGarr limit versus tectonic statistical limit (based on databases of Evans et al., 2012; McGarr, 2014)

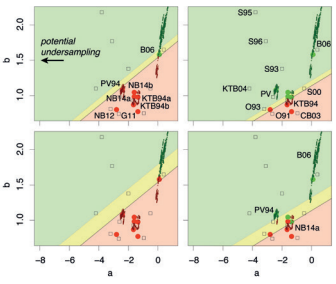

(*a*,*b*) scattering versus TLS pass/fail for different *Q* and *d* (modified from Mignan et al., in rev.)

- Fatality curves & probability of TLS failure p:

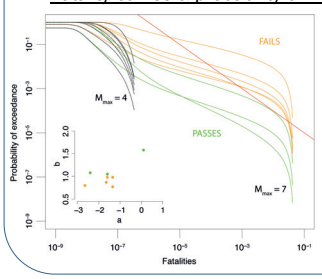

✓ d = 10 km from nearest building

✓ All M_{max} = 4 scenarios pass

✓ 5/8 M_{max} = 7 scenarios fail

✓ Yields p = (0+5)/16 ≈ 0.3

- Probability p & price changes versus distance to nearest habitation:

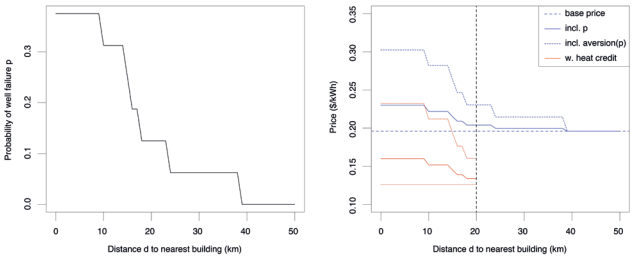

✓ Probability p decreases relatively fast with increasing distance d
✓ For maximum p (at d=0), the price increases from 0.20 to 0.23$/kWh
✓ Including risk aversion via CPT, the price increases to 0.30$/kWh
✓ A heat credit of 0.07$/kWh at short distances tends to compensate the increase, indicative of a trade-off between heat credit & seismic risk

Discussion

Advantages of the approach:
✓ Transparent actuarial approach, via TLS-based mitigation strategy
✓ Translates cost of seismic risk mitigation into electricity price
✓ To the public: Assured that a fixed safety threshold is respected
✓ To the industry: Decision making under uncertainty made possible
✓ To the authorities: Improved decisions based on clear rules. If the cost of failed wells becomes too high for the EGS industry, authorities may decide to decrease the safety threshold. E.g., for 10^{-5} probability of fatality, the original base price is reached at 5km

The additional cost of ambiguity:
✓ max(M_{max}) critical to probability of failure. Could be reduced if the underground was better known
✓ A 0.5 probability for max(M_{max}) is disputable (*Bommer & van Elk*, 2017). Whatever value used, ambiguity must be discussed in terms of a stress test (minimax option where the worst possible scenario is investigated)
✓ Reduction of uncertainties is costly & may not decrease risk
✓ Passing a stress test may be costly due to e.g., building retrofitting

Limitations:
✓ **All values and graphs shown here are subject to the modelling and parameter choices**
✓ Damage of potential earthquakes not considered & assumed insured
✓ (*a*,*b*) parameter set assumed independent of location. However if one well fails, e.g. due to high *a*-value, it is plausible that nearby wells would react in a similar way, meaning an increase of p

References

Bommer & van Elk (2017), about: Workshop on Maximum Magnitudes for Groningen, Bull. Seismol. Soc. Am. 107
Evans et al. (2012), A survey of the induced seismic response to fluid injection in geothermal and CO_2 reservoirs in Europe, Geothermics 41
Lacirignola & Blanc (2013), Environmental analysis of practical design options for EGS through life-cycle assessment, Renewable Energy 50
McGarr (2014), Maximum magnitude earthquakes induced by fluid injection, J. Geophys. Res. 119
Mignan et al. (2015), Induced seismicity risk analysis of the 2006 Basel, Switzerland, EGS project: Influence of uncertainties on risk mitigation, *Geothermics* 53
Mignan et al., Induced seismicity closed-form traffic light system for actuarial decision-making during deep fluid injections, Sci. Rep. (in rev.)
Hirschberg et al. (2015), Energy from the Earth, TA Swiss 62
Tversky & Kahneman (1992), Advances in Prospect Theory: Cumulative Representation of Uncertainty, J. Risk Unc. 5

SCCER SoE
SWISS COMPETENCE CENTER for ENERGY RESEARCH
SUPPLY of ELECTRICITY

SCCER-SoE Annual Conference 2017

In cooperation with the CTI
Energy
Swiss Competence Centers for Energy Research
Schweizerische Eidgenossenschaft
Confédération suisse
Confederazione Svizzera
Confederaziun svizra
Swiss Confederation
Commission for Technology and Innovation CTI

Monitoring and imaging medium perturbations using multiply scattered waves

Anne Obermann, Thomas Planès, Céline Hadziioannou, Michel Campillo, Stefan Wiemer

Context of the work

Changes in the seismic waveform between two perfectly reproducible acquisitions can be attributed to variations of elastic properties in the evolving medium. In mainly homogeneous lithologies, strong medium changes might be detected by direct waves, however, their sensitivity to weak changes is low. The **seismic coda**, the product of multiple scattering processes caused by heterogeneities, samples the propagation medium very densely, resulting in a high sensitivity to tiny modifications of the seismic properties in the medium. This sensitivity has been successfully used for monitoring purposes in different areas of seismology, among them the application to the deep geothermal ernergy projects in St. Gallen (Obermann et al. 2015) and Basel (Hillers et al. 2015), where additional information about the reservoir dynamics could be obtained.
Besides the **detection** of medium changes, an important aspectthe seismic is their **location** in space. The diffusive wave propagation in the seismic coda needs to be approximated in a probabilistic way. Based on the radiative transfer theory, we developed 2D and, recently, 3D probablistic sensitivity kernels to image the changes in space. The 3D kernels are successfully applied in numerical simulations to accurately determine the depth of the medium changes.

Detection of medium changes

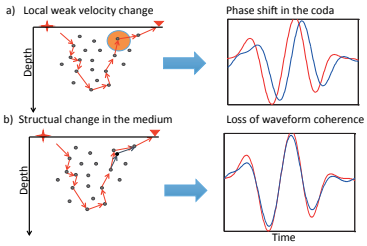

We compare a waveform of the seismic coda prior to a medium change (in blue) to waveforms affected by different kinds of changes (in red).
For this type of study we need perfectly reproducible acquisitions, depending on the scale (frequency), we use ambient noise cross-correlations (passive source) or active sources.

Application to the deep geothermal project in St. Gallen

In 2012, the project in St. Gallen targeted a hydrothermal resource at a depth of 3.5–5 km. Minor injection tests and acid stimulations showed low levels of micro seismicity. A sudden gas leakage into the well came as a surprise. Well rescue operations led to a ML 3.5 earthquake. Was there an aseismic response of the reservoir to the injections that could have alarmed operators?

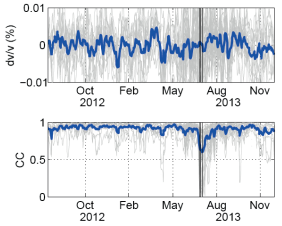

We calculate daily cross-correlations from the ambient seismic noise recordings and search the seismic coda (averaged over all station couples) for time-lapse changes. The vertical lines indicate the injection tests. You notice a clear waveform decoherence (CC), while there is no noticeable velocity change (dv/v).

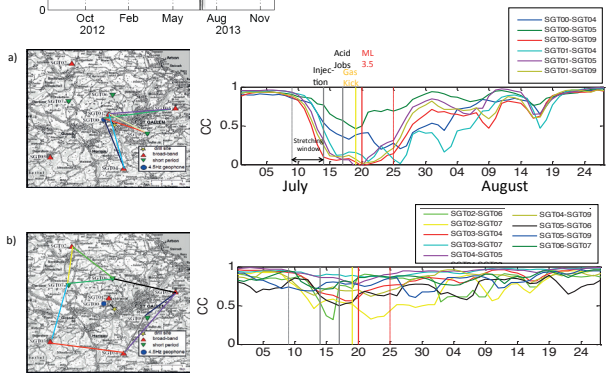

We zoom into the injection period and focus on the individual station pairs. Station pairs close to the injection well (a) noticed a waveform perturbation with the onset of the injections, while others did not (b). We interpret the massive loss of coherence as gas penetrating into the formation as a consequence of the injections and acid jobs.
Continuous monitoring with coda waves can provide additional information on aseismic reservoir processes that cannot be resolved with standard seismic analysis.

Location of the changes (St. Gallen)

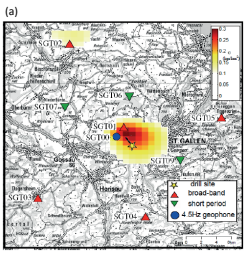

Horizontal location of the medium perturbation with an inversion procedure (a) based on 2D probabilistic approaches (Obermann et al. 2013). The medium perturbations can be confined within a few hundred meters of the injection well.
For the vertical location, we used a **spectral analysis**. The highest amount of coherence loss is found between 0.2-0.4 Hz (b). These frequencies are sensitive to the Malm layer where the injection occurred (c). Due to the nonuniform excitation of the ambient seismic field, a spectral analysis remains very approximative.

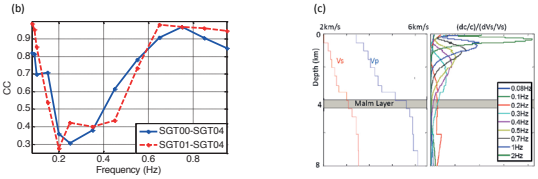

Development of 3D probabilistic kernels and numerical performance testing

We simulate coda waves in a heterogeneous model (a) with and without a cubic velocity perturbation. We developed 3D probabilistic sensitivity kernel (b) as a combination of bulk and surface wave sensitivity and successfully used them to locate the velocity perturbations at depth (c).

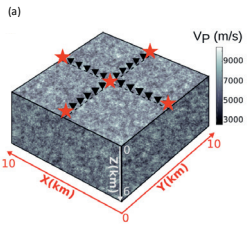

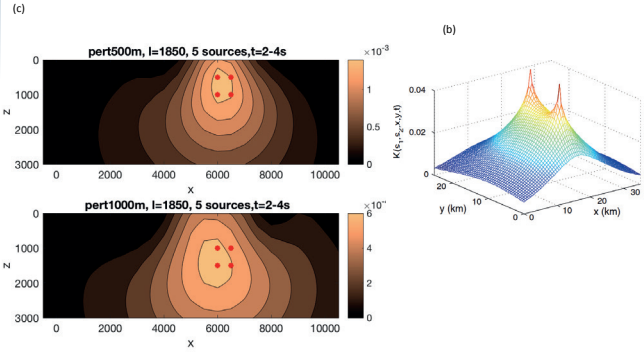

Imaging with such probabilistic 3-D kernels that are critical for depth location, could significantly improve our understanding of the nature of the medium variations revealed by seismic monitoring.

Next steps

Application of the 3D probabilistic kernels to real data sets (Basel, St. Gallen, Grimsel).
Further theoretical developments to accurately describe the elastic case.

References

Obermann et al. (2013) Imaging pre- and co-eruptive structural and mechanical changes on a volcano with ambient seismic noise, JGR, 118.
Obermann et al. (2015) Potential of ambient seismic noise techniques to monitor reservoir dynamics at the St. Gallen geothermal site. JGR, 120 (6).
Obermann et al. (2016) Lapse-time dependent coda wave depth sensitivity to local velocity perturbations in 3-D heterogeneous elastic media, GJI, 207.
Hillers et al. (2015) Noise based monitoring and imaging of aseismic transient deformations induced by the 2006 Basel reservoir stimulations, Geophysics, 80, 4.

SCCER-SoE Annual Conference 2017

SCCER SoE
SWISS COMPETENCE CENTER for ENERGY RESEARCH
SUPPLY of ELECTRICITY

In cooperation with the CTI
Energy
Swiss Competence Centers for Energy Research
Schweizerische Eidgenossenschaft
Confédération suisse
Confederazione Svizzera
Confederaziun svizra
Swiss Confederation
Commission for Technology and Innovation CTI

PAUL SCHERRER INSTITUT
PSI

A preliminary Spatial Multi-Criteria Decision Analysis for Deep Geothermal Systems in Switzerland

Matteo Spada, Peter Burgherr
Technology Assessment Group, Laboratory for Energy Systems Analysis, Paul Scherrer Institut (PSI)

Introduction

This study presents a preliminary application of a spatial Multi-Criteria Decision Analysis (sMCDA) to Deep Geothermal Energy (DGE) systems in Switzerland. sMCDA is a tool that combines Geographical Information Systems (GIS) capabilities with MCDA frameworks to take into account the spatial dimension, which is important for planning and decision-making purposes, etc. [1].

The scope of this work is to assess the most sustainable area for a hypothetical DGE plant in Switzerland. The focus is on the Molasse basin, Rhine Graben, and Jura mountains regions (i.e., not the Alpine region) where most of the Swiss DGE projects are planned. The proposed approach combines spatial information from both explicit data (e.g., heat flow) and calculated ones (e.g., risk indicators, environmental impact indicators, etc.) for specific *a priori* defined plant characteristics (e.g., capacities, number of drilled wells over lifetime). Results are then presented for different hypothetical preference profiles.

Method

The sMCDA framework consists of different steps. First, the characteristics of the technology to be used in the sustainability assessment has been selected. In this study, since no running DGE plants exist in Switzerland, an hypothetical power plant based on SCCER-SoE Phase 1 activities is considered (Table 1).

Table 1: Key physical parameters of the DGE plant capacity case considered in this study

Model Assumption	Unit	Value
Net Plant Capacity	MWe	1.47
Annual Generation	MWh/year	11849
Life Time	years	20
Number of Wells		2
Well Depth	km	5
Well Life Time	year	20

Next, criteria are established to cover all 3 pillars of sustainability (environment, economy and society). Furthermore, indicators are chosen for each criterion based on availability and potential spatial variability (Table 2).

Table 2: Selected criteria and indicators used in this study.

Criteria	Indicators	Unit
Environment	Climate Change	kg CO2 eq to air
	Human Toxicity	kg 1,4-DCB eq to urban air
	Particulate Matter Formation	kg PM10 eq to air
	Water Depletion	m3 (water)
	Metal Depletion	kg Fe eq
Economy	Average Generation Cost	rp/kWhe
Society	Non-seismic Accident Risk	Fatalities/kWh
	Natural Seismic Risk	Ordinal Scale [1-3]

Indicators are then quantified for the hypothetical plant in Table 1 and for a set of 31 potential areas defined using Heat Flux and Natural Seismic Risk maps (https://map.geo.admin.ch). Environmental and economic indicator values have been estimated based on the temperature gradient (ΔT) in the area of interest, since ΔT is the ratio between the HF and the thermal conductivity of rocks (on average 3 W/m*°C in Switzerland [2]). On the other hand, the non-seismic accident risk indicator considers blow out risk and release of selected hazardous chemicals, which are related to the number of drilled wells [3]. The natural seismic risk indicator is considered in this study as a proxy of social acceptance, meaning that high risk is associated with lower social acceptance of a DGE system.

Once estimated, indicators are normalized to express them in a unit-less scale so they can be combined. Afterwards, they are weighted, based on individual stakeholder preferences. Finally, the indicators are aggregated using the weighted sum algorithm (WSA), which has been chosen due to its simplicity and transparency, for each area to receive a sustainability index for ranking purposes.

Results

No stakeholder interaction, e.g., through elicitation, has been performed in this study to assess weighting profiles of "real world" stakeholders. Instead, four artificial preference profiles have been defined:

- equal weights at all levels (both criteria and indicators in Table 2), which corresponds to the spirit of sustainability, where all pillars have the same weight.
- three weighting profiles that strongly favor one of the sustainability pillars (weight 80%), whereas the two other are both weighted 10%, and all indicators are equally weighted.

As an example, the results of the profile focusing on the Environment (80%) are shown in Figure 1. The lower the sMCDA score is in the figure, the better the area performs in terms of sustainability. From Figure 1a, the most sustainable areas are the ones in NE Switzerland. Furthermore, Figure 1b shows the contributions of each indicator to the final result. In particular, results for areas with highest values (e.g., 2) are strongly affected by the environment related indicators only, while the ones for areas with lower values (e.g., 17) are more a combination among the different indicators in Table 2.

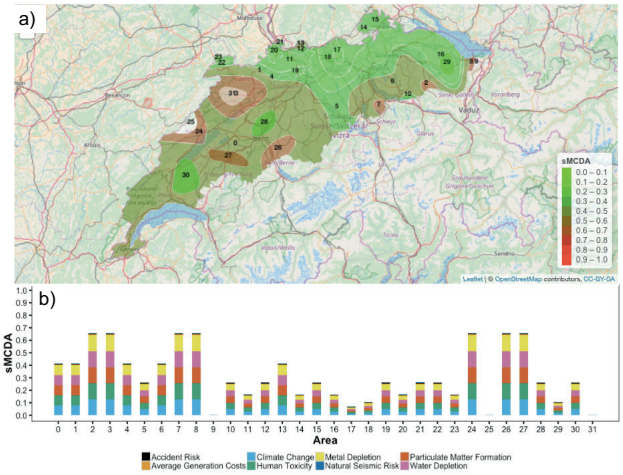

Figure 1: Environment-focused profile. a) Spatial distribution of the sMCDA results for Switzerland. b) Indicator contributions to each area.

Conclusions

- First application of sMCDA to DGE in Switzerland and its suitability as a decision-support tool has been demonstrated.
- Equal weighting generally leads to lower scores than preference profiles favoring a particular sustainability dimension.
- Rankings of profiles focusing on environment and economy are practically the same, but the indicator contributions differ. Generally, areas in NE Switzerland perform best.
- When focusing on social indicators, only few area have low sustainability scores, i.e. all areas along the basin are competitive, except for few in the North.

References

[1] Ferretti, V. & Montibeller, G. 2016. Key challenges and meta-choices in designing and applying multi-criteria spatial decision support systems. *Decision Support Systems*, 84, 41-52. doi: http://dx.doi.org/10.1016/j.dss.2016.01.005

[2] Bodmer Philippe H., (1982): Beiträge zur Geothermie der Schweiz. Diss. Naturwiss. ETH Zürich, Nr. 7034, 210 p.

[3] Spada, M., Burgherr, P. (2015). Chapter 6.1: Accident Risk. In Hirschberg S., Wiemer S. and Burgherr P.: Energy from the Earth. Deep Geothermal as a Resource for the Future? TA-SWISS Study TA/CD 62/2015, vdf Hochschulverlag AG, Zurich, Switzerland, pp. 229-262. http://dx.doi.org/10.3218/3655-8.

SCCER SoE
SWISS COMPETENCE CENTER for ENERGY RESEARCH
SUPPLY of ELECTRICITY

SCCER-SoE Annual Conference 2017

FNSNF
SWISS NATIONAL SCIENCE FOUNDATION

Building informed and realistic public preferences for Swiss electricity portfolios

Sandra Volken, Georgios Xexakis, Evelina Trutnevyte,
ETH Zurich, Department of Environmental Systems Science (USYS), USYS Transdisciplinarity Lab

Background

- Public debates about electricity generation as well as scientific studies usually focus on individual technologies[1,2,3,4].
- The public thus might neglect that electricity needs to be generated by a portfolio of technologies and that each technology comes with diverse risks and operational impacts to public health, safety, natural and built environment[5,6].
- We thus also know little about electricity portfolio preferences, even though we assume that also non-experts think of electricity generation as an interconnected system[7].
- Previous research shows that both group deliberation and targeted information can help formation of informed preferences [8,2,3]. We thus study such realistic electricity portfolio preferences for the first time for a sample of informed Swiss laypeople.

Research questions:

1. What are the public preferences for Swiss electricity generation, given balanced information on technology risks and operational impacts?
2. How do these informed preferences differ if the technologies are considered individually or if they need to be combined into realistic portfolios for Switzerland?
3. What is the short and longer-term effectiveness of different formats of information and deliberation on
   a) technology preferences and characteristics,
   b) revealed and self-rated knowledge, and
   c) willingness-to-act and interest in the energy topic, in the?
4. What is the usability and usefulness of information materials and how satisfied are participants with factsheets, Riskmeter, and workshops?

Methods and Materials

1. Invitation of 55 diverse laypeople to online survey #1 (Fig. 1) based on registration survey (demographics and technology preferences)
2. Homework: reading of factsheets (Fig. 2+3), containing tailor-made and comparable information about 13 technologies and 9 impact categories.
3. Participation of informed laypeople (N=46) in one of four workshops: discussing in small groups, submitting a portfolio created with the interactive web-tool Riskmeter (see Fig.4), and completing several paper-and-pencil surveys (#2-#5) (Fig 1).
4. Follow-up online survey (#6) after four weeks (Fig. 1).

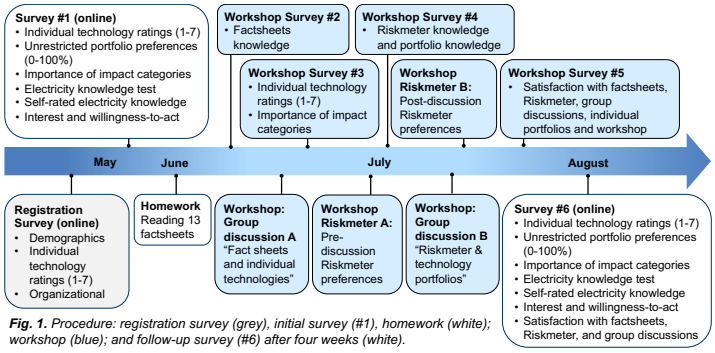

Fig. 1. Procedure: registration survey (grey), initial survey (#1), homework (white); workshop (blue); and follow-up survey (#6) after four weeks (white).

Results

- We found highest support for low-carbon technologies: solar cells, electricity savings, waste incineration and all types of hydro power.
- Portfolio preferences (Fig. 4) complete individual technology ratings (see Fig. 5) in understanding public preferences.
- The impact of information on preferences (Fig. 5) depends on the type of measurement and technology. However, the longer-term influence remains unclear.
- We found a positive effect of information and workshops on electricity knowledge and self-rated knowledge.
- Participants were satisfied with and understood factsheets (Fig. 2+3) and Riskmeter (Fig. 4).
- Most important impact categories (Fig. 2) were climate change, local air pollution, and electricity supply reliability.

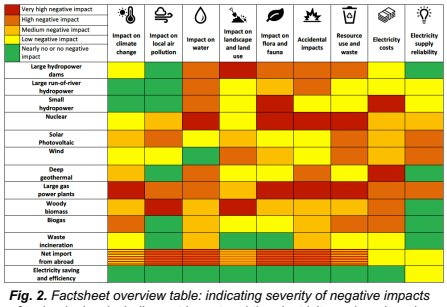

Fig. 2. Factsheet overview table: indicating severity of negative impacts of technologies, including net import and the electricity savings (rows), on different impact categories (columns). From dark red (= very high negative impact) to green (= no or negligible negative impact).

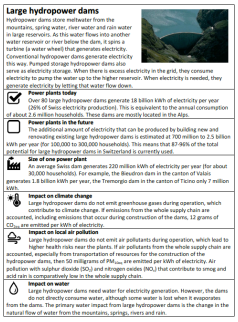

Fig. 3. Factsheet example: Large Hydro Dams (page 1/2).

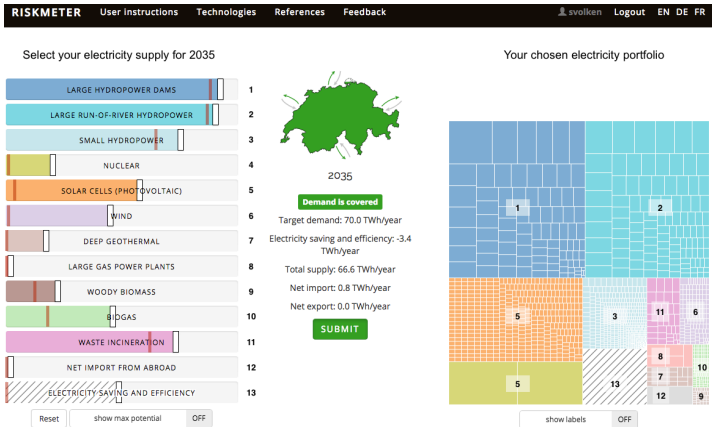

Fig. 4. Adaptation from the interactive-online tool RISKMETER (www.riskmeter.ethz.ch), showing the average portfolio selected by participants. Mean TWh/year and SD in decreasing order: Large hydro dams (20.3±1.1), large run-of-river hydropower (18.7± 1.0), solar cells (11.3±5.7), nuclear (5.0±8.0), small hydropower (4.5±0.9), electricity savings (3.7±2.5), waste incineration (2.7±0.5), wind (2.0±1.5), large natural gas (1.0±2.5), net import (0.9±3.4), deep geothermal (0.8±1.3), biogas (0.7±0.4), woody biomass (0.3±0.3). On the left: available potential and TWh/year selected for each technology, the red line indicates the initial position. Right: Portfolio in TWh/year out of selected technologies.

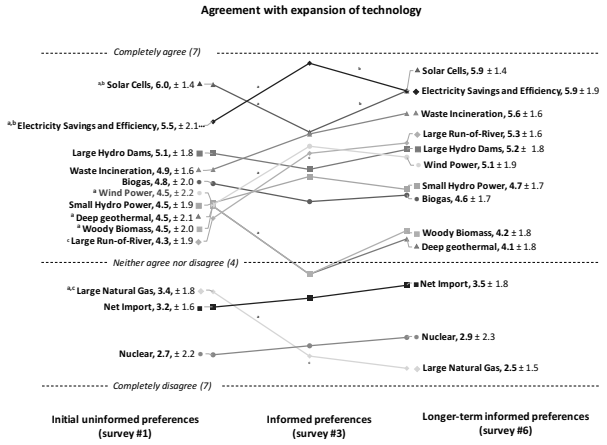

Fig. 5. Preferences for electricity generation technologies (7-point Likert scale ranging from 1= completely disagree to 7= completely agree with expansion of power plants until 2035). Significant ($p < 0.05$) difference between: [a] initial preferences (left) and informed preferences (middle); [b] informed preferences (middle) and longer-term preferences (right); [c] initial (left) and longer-term (right) preferences.

References

[1] Demski C, Butler C, Parkhill KA, Spence A, Pidgeon NF. Public values for energy system change. Global Environmental Change. 2015;34:59-69.
[2] Fleishman LA, De Bruin WB, Morgan MG. Informed public preferences for electricity portfolios with CCS and other low-carbon technologies. Risk Anal. 2010;30(9):1399-410.
[3] Trutnevyte E, Stauffacher M, Scholz RW. Supporting energy initiatives in small communities by linking visions with energy scenarios and multi-criteria assessment. Energy Policy. 2011;39(12):7884-95.
[4] Pidgeon N, Demski C, Butler C, Parkhill K, Spence A. Creating a national citizen engagement process for energy policy. Proc Natl Acad Sci U S A. 2014;111 Suppl 4:13606-13.
[5] Sovacool BK, Andersen R, Sorensen S, Sorensen K, Tienda V, Vainorius A, et al. Balancing safety with sustainability: assessing the risk of accidents for modern lowcarbon energy systems. Journal of Cleaner Production. 2016;112:3952-65.
[6] Hirschberg S, Bauer C, Burgherr P, Cazzoli E, Heck T, Spada M, et al. Health effects of technologies for power generation: Contributions from normal operation, severe accidents and terrorist threat. Reliability Engineering & System Safety. 2016;145:373-87.
[7] Volken S., Wong-Parodi G., Trutnevyte E. 2017. Public awareness and perception of environmental, health and safety risks related to electricity generation: An explorative interview study in Switzerland. Under review.
[8] Mayer LA, Bruine de Bruin W, Morgan MG. Informed public choices for low-carbon electricity portfolios using a computer decision tool. Environ Sci Technol. 2014;48(7):3640-8.

SCCER SoE
SWISS COMPETENCE CENTER for ENERGY RESEARCH
SUPPLY of ELECTRICITY

SCCER-SoE Annual Conference 2017

FNSNF
SWISS NATIONAL SCIENCE FOUNDATION

Are Interactive Web-Tools for the Public Worth the Effort?
An Experimental Study on Public Preferences for the Swiss Electricity System Transition

Georgios Xexakis, Evelina Trutnevyte

ETH Zürich, Department of Environmental Systems Science (USYS), USYS Transdisciplinarity Lab

Introduction

Interactive web-tools is a recent trend in scientific communication (Spiegelhalter et al. 2011; Trutnevyte & Fuss 2017). They are often regarded as powerful methods to create engaging and personalized stories out of complex data, beyond the framing of static information (Grainger et al. 2016). In many fields, including environmental, climate and energy sciences, they are used as a solution for effective communication (McInerny et al. 2014; Parsons & Sedig 2011) and decision aids for the wider public (Aye et al. 2015; Bessette et al. 2014; Gong et al. 2017; Trutnevyte & Fuss 2017).

Nevertheless, including interactivity is much more resource consuming than traditional methods and, in some cases, may even undermine or complicate the communication further (Zikmund-Fisher 2012; Wong-Parodi et al. 2014). Although studies exist on how to design and assess interactive web-tools (Wong-Parodi et al. 2014), there is little empirical evidence whether they are more effective in communicating the messages, in comparison with more traditional methods (Zikmund-Fisher et al. 2011).

We study this effect in performance in the case of the Swiss electricity supply system transition to 2035 and specifically the elicitation of preferences from non-experts, given the information on health, safety, built and natural environment risks. This case study is considered appropriate as it involves a multidimensional and complex problem, i.e. a large number of possible transition strategies (Berntsen & Trutnevyte 2017) along with their aforementioned risks, that also generates interest and concern to the Swiss society, as shown by the recent votes for the Nuclear Phase-out and the Energy Strategy 2050.

Research questions

1. How do interactive and static formats of information perform in terms of making this information understandable, trustworthy and interesting for non-experts?
2. Is there a difference between a subjective and objective measurement of this performance?
3. Does the format affects the active mastery of the information?
4. In the case of informing non-experts for the health, safety, built and natural environment risks of the Swiss electricity supply system transition, does the format type affects the willingness to act on energy issues, the general interest in energy issues and the technology preference?

Methods and materials

We will conduct an experimental online survey with two groups (N=400 in total), where each group receives the same information on electricity supply technologies and strategies (Table 1), portfolios of these technologies and strategies, and associated impacts and risks (Table 2). The two groups will differ in the format of information: a static format (Figure 1), using text descriptions and static visualizations of four maximally different portfolios, and an equivalent interactive format (Figure 2), using a web-based RISKMETER tool we have developed (accessible at https://riskmeter.ethz.ch). Both groups will be asked to answer the same questions in the survey, including the questions on dependent variables (Table 3) as well as questions on demographic data, digital literacy, previous energy interest and understanding, to be used for experimental check.

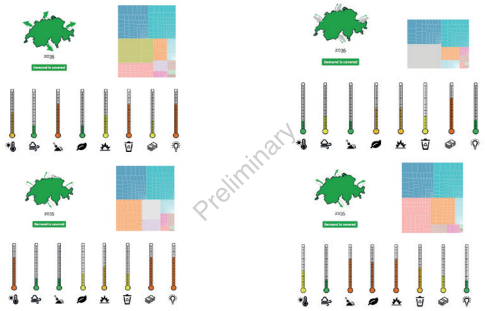

Figure 1. Static format – four maximally different portfolios

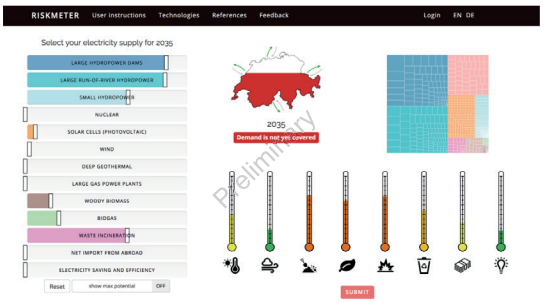

Figure 2. Interactive format – RISKMETER (accessible at https://riskmeter.ethz.ch)

• Large hydropower dams	• Large gas power plants
• Large run-of-river hydropower	• Woody biomass
• Small hydropower	• Biogas
• Nuclear	• Waste incineration
• Solar cells (photovoltaic)	• Net import from abroad
• Wind	• Electricity saving and efficiency
• Deep geothermal	

Table 1. Electricity supply technologies and strategies

Criteria	Measurement
Impact on climate change	g $CO_{2\text{-eq}}$/kWh
Impact on local air pollution	mg PM_{10eq}/kWh, mg SO_2/kWh, mg NO_x/kWh
Impact on water	water withdrawal in m^3/kWh, water discharge temperature in ºC, water discharge effluents
Impact on landscape and land use	m^2/kWh
Impact on flora and fauna	PDF*m^2*a/kWh (ecosystem quality)
Accidental impacts	fatalities/kWh, fatalities/accident
Resource use and waste	mg solid waste/kWh, renewable and non-renewable primary energy equivalent in MJ-eq/kWh_{el}
Electricity costs	Rp/kWh
Electricity supply reliability	resource supply (0-10), flexibility (0-10)

Table 2. Criteria for health, safety, built and natural environment risks

Dependent variables	Measurement	
	Subjective	Objective
Understandability	Direct question(s)	True or false question(s) relying on given information
Interest	Direct question(s)	Time spent, completion rate
Trust	Direct question(s)	*Under discussion*
Active mastery	*Under discussion*	True of false question(s) requiring inferences on given information
Willingness to act on energy issues	Direct question(s)	*Under discussion*
Interest in energy issues	Direct question(s)	*Under discussion*
Technology preference	Direct question(s)	*Under discussion*

Table 3. Dependent variable measurement in the survey

Expected results

- We hypothesize that the non-expert users will be more interested and engaged with the interactive than with the static format.
- We are not expecting statistically significant differences of trust between the two formats but we cannot exclude the possibility that participants might perceive interactive tools more as games and less as tools, disregarding thus the significance of the information.
- We are expecting a difference between the subjective and the objective measurement of performance, especially in the understanding of the interactive format: participants might be overwhelmed by the higher information availability and the exploration freedom of this format, leading possibly to a lower objective measurement of understanding.

References

Aye, Z. et al., 2015. Prototype of a Web-based Participative Decision Support Platform in Natural Hazards and Risk Management. *ISPRS International Journal of Geo-Information*, 4(3), pp.1201–1224.

Berntsen, P.B. & Trutnevyte, E., 2017. Ensuring diversity of national energy scenarios: Bottom-up energy system model with Modeling to Generate Alternatives. *Energy*, 126, pp.886–898.

Bessette, D.L., Arvai, J. & Campbell-Arvai, V., 2014. Decision support framework for developing regional energy strategies. *Environmental Science & Technology*, 48(3), pp.1401–1408.

Gong, M. et al., 2017. Testing the scenario hypothesis: An experimental comparison of scenarios and forecasts for decision support in a complex decision environment. *Environmental Modelling and Software*, 91, pp.135–155.

Grainger, S., Mao, F. & Buytaert, W., 2016. Environmental data visualisation for non-scientific contexts: Literature review and design framework. *Environmental Modelling and Software*, 85, pp.299–318.

McInerny, G.J. et al., 2014. Information visualisation for science and policy: engaging users and avoiding bias. *Trends in Ecology & Evolution*, 29(3), pp.148–157.

Parsons, P. & Sedig, K., 2011. Human-information interaction: An emerging focus for educational cognitive tools. *Education in a technological world: communicating current and emerging research and technological efforts*, pp.245–251.

Spiegelhalter, D., Pearson, M. & Short, I., 2011. Visualizing Uncertainty About the Future. *Science*, 333(6048), pp.1393–1400.

Trutnevyte E., Fuss, G. 2017. Review of web-based interactive tools and decision aids for long-term energy transition, under preparation.

Wong-Parodi, G., Fischhoff, B. & Strauss, B., 2014. A method to evaluate the usability of interactive climate change impact decision aids. *Climatic Change*, 126(3–4), pp.485–493.

Zikmund-Fisher, B.J., 2012. The Right Tool Is What They Need, Not What We Have: A Taxonomy of Appropriate Levels of Precision in Patient Risk Communication. *Medical Care Research and Review*, 70, pp.1–23.

Zikmund-Fisher, B.J., Dickson, M. & Witteman, H.O., 2011. Cool but counterproductive: Interactive, web-based risk communications can backfire. *Journal of Medical Internet Research*, 13(3), pp.1–11.